lncRNA (Mao et al, 2011). The expression of NEAT1 and Malat1 lncRNA, both of which have multiple TDP-43 binding sites, is elevated in FTLD-TDP brain (Tollervey et al, 2011). Our study with FTLD-TDP patients also demonstrated an increased expression level of NEAT1 (Supporting Information Fig S6B and D). However, NEAT1 was not significantly altered in ALS spinal cord and TDP-43 depleted cells (Supporting Information Fig S6A and C), suggesting distinct regulations of this lncRNA in different disease conditions. Nevertheless, the enrichment of TDP-43 in paraspeckles and speckles should be examined further to determine any potential role in RNA metabolism in these nuclear subdomains. Taken together, the expression of U snRNA spliceosome components was aberrant and long non-coding RNAs were normal in ALS spinal cords, but these profiles were reversed in FTLD. These results suggest that while neurodegenerative diseases with distinct causal genes (ALS, SMA) can have disruptions in a common biochemical pathway, diseases with the same causal gene (ALS, FTLD) can also have disruptions in distinct pathways.

In conclusion, we show here that TDP-43 and SMN share a common function in spliceosomal U snRNP biogenesis. Dysfunction of these distinct proteins in ALS and SMA leads to collapse of spliceosome integrity and abnormal splicing in motor neurons. We expect that further investigation of defects in RNA metabolism common to these motor neuron diseases but different from a related brain disease should provide explanation to the cell-type specific vulnerability observed in neurodegenerative diseases. In addition, targeting spliceosome and/or Gem stability in motor neurons may represent a new class of candidate therapeutics for motor neuron diseases.

MATERIALS AND METHODS

Expression vectors

The open reading frame of human *TARDBP* was inserted into p3XFLAG-CMV14 vector (Sigma), resulting in the insertion of an 18 amino acid spacer between the TDP-43 C-terminus and 3XFLAG peptides. Coding regions of TDP-43 fused with 3xFLAG were subcloned into pF5K-CMV-neo vector (Promega). For FUS/TLS expression, the open reading frame of human *FUS/TLS* fused with 3XFLAG on its N-terminus were subcloned into pF5K-CMV-neo or pF5A-CMV-neo vector (Promega).

Cell culture and immunofluorescence

Hela cells were maintained in DMEM with high glucose (Gibco) supplemented with L-glutamine, and 10% foetal bovine serum (Gibco). SH-SY5Y cells were maintained in Advanced DMEM/F12 (Gibco) with non-essential amino acids, sodium pyruvate, GlutaMAX (Gibco), and 10% foetal bovine serum. Hippocampal neurons were isolated from E16.5 C57BL6 or $FUS^{-/-}$ mouse embryos and cultured essentially as described (Huang et al, 2007). Cells were cultured on chamber slides (Lab-Tek, Nunc), fixed with 4% paraformaldehyde for 10 min and permeabilized with 0.1% Triton X-100. For paraspeckle staining with mouse anti-p54 (BD transduction), cells were fixed with cold methanol. Non-specific binding was blocked by incubation with 1% normal goat serum prior to the application of primary antibody. Antibodies used were as follows: rabbit anti-TDP-43 (ProteinTech), anti-coilin (Sigma, clone pδ), mouse anti-p54 (BD transduction), anti-SRSF2 (Sigma, clone SC-35), mouse anti-SMN (BD transduction, 610646), rabbit anti-SMN (Santa Cruz, sc-15320), mouse anti-Gemin8 (Santa Cruz, sc-130669), rabbit anti-FUS/TLS (Abcam, 70381), anti-dimethylated Sm proteins (Lab Vision Corp./Thermo Scientific, clone Y12), anti-TMG (Santa Cruz, clone K121), mouse anti-FLAG (M2), rabbit anti-FLAG (Sigma) and rabbit anti-GFP (MBL).

Knockdown of protein expression in cells

To eliminate TDP-43 expression, Hela cells were transfected with 4 nM Stealth siRNA for *TARDBP* (Invitrogen, ID#HSS177422 or originally designed oligos with the sequences listed in Supporting Information Table S2) or control siRNA (Invitrogen, LoGC#2 or #3) in suspension at 1.5×10^5 cells/ml using Lipofectamine RNAiMax (Invitrogen). After an overnight culture, cells were then transfected with siRNA once more, and then cultured for two more days. For SH-SY5Y cells, cells were transfected in suspension at 3×10^5 cells/ml. After 3 days of culture, cells were divided into three dishes, transfected with siRNAs again and cultured for three more days.

Immunoprecipitation

Cells were transfected with pF5K-TDP-43-3xFlag constructs using X-tremeGENE HP (Roche). Cells were harvested and washed with PBS 3 times. TBS supplemented with 0.2% Triton X-100, protease inhibitors (Nakalai, Japan), and RNase inhibitor SUPERase-In (Ambion) was used as a Lysis buffer. The cell pellet was then lysed in the same volume of Lysis buffer on ice for 10 min. The nuclear membrane was disrupted by passage through a 28 G needle and then centrifuged at 14,000*g* for 15 min. Supernatants were collected as total cell extracts. After the protein concentration of cell extracts was adjusted to 5–8 mg/ml with Lysis buffer, cell extracts were mixed with agarose beads conjugated with anti-FLAG antibody (M2-agarose, Sigma) and incubated overnight at 4°C. After washing with Lysis buffer for three times, non-specific protein binding to the anti-FLAG agarose beads was washed out by incubating with FLAG peptide at 50 μg/ml for 15 min at 4°C. This step was critical to wash out non-specific or weak binding to the anti-FLAG agarose beads. To elute the protein complex with 3XFLAG-tagged protein, 3XFLAG peptides were added to the agarose beads at 500 μg/ml and incubated for 1 h at 4°C. Eluted proteins were then analysed by immunoblotting. For immunoprecipitation of HA-tagged protein, anti-HA-agarose (Sigma) was used instead of anti-FLAG agarose, and the precipitated proteins were eluted with SDS-sample buffer.

For immunoprecipitation of mature U snRNPs, a nuclear pellet was obtained from suspension cells using Buffer A (50 mM Hepes pH 7.5/1 mM $MgCl_2$/1 mM EGTA/1 mM DTT/protease inhibitors) on ice for 10 min followed by centrifugation at 3000*g* for 5 min. The nuclear pellet was lysed in Buffer A supplemented with 150 mM KCl, 1% NP-40, 10% glycerol, and RNase inhibitor SUPERase-In (Ambion) and then the nuclear membrane was disrupted by passage through a 27 G syringe 10 times and a repeated freeze/thaw cycle 3 times. Nuclear extract was obtained after the removal of cell debris by centrifugation at 20,000*g* for 10 min. Anti-Sm proteins monoclonal antibody (Y12) and mouse immunoglobulin (as negative control) were used for immunoprecipitation. Antibodies used for Western

The paper explained

PROBLEM:

The motor neuron diseases (ALS) and spinal muscular atrophy (SMA) are caused by dysfunction of proteins involved in RNA metabolism. For ALS, the RNA-binding proteins TDP-43 and FUS/TLS, have been implicated, while in SMA the protein SMN, essential for biogenesis of spliceosomal component snRNPs, is critical. A key question is whether there is a shared defective mechanism in RNA metabolism common to these two diseases.

RESULT:

We report a convergent function for TDP-43, FUS/TLS and SMN by showing that the genes for these diseases share a common mechanism: maintenance of nuclear Gems and controlling the level of U snRNA spliceosomal complex. In ALS spinal motor neurons as well as TDP-43 depleted neurons, we observed disruption of Gems and abnormal accumulation of U snRNAs/snRNPs. Together, our findings indicate that TDP-43, FUS/TLS and SMN are important for spliceosome integrity, and that collapse of the spliceosome is the critical mechanism that must underlie the neurodegenerative process in both ALS and SMA.

IMPACT:

Our study reveals the important role of nuclear Gems and spliceosomal U snRNPs in motor neuron survival. Although it requires more investigation, our work substantially contributes to understanding the molecular mechanism of motor neuron disease by providing evidence linking for the first time the selective vulnerability of motor neurons to spliceosome breakdown in Gems of ALS and SMA. Furthermore, targeting spliceosome and/or Gem stability in motor neurons may represent a new class of candidate therapeutics for motor neuron diseases.

blot were as follows: mouse anti-FUS/TLS (Santa Cruz, sc-47711), rat anti-PRPF3 (MBL, clone 4E3), goat anti-U1-70K (Santa Cruz), mouse anti-PABP (Sigma, clone 10E10) and rabbit anti-eIF4G (Cell Signaling, #2498).

FUS/TLS knockout mice

ES cell clone (HMA274) with β-Gal-neo cassette inserted between exon 2 and 3 of *FUS/TLS* gene were obtained from mutant mouse regional resource centers at University of California, Davis, and used to generate FUS/TLS heterozygous mice with support by Research Resource Center of RIKEN Brain Science Institute. Genotyping of mice with disrupted FUS/TLS allele was performed using RT-PCR, and FUS/TLS protein levels were confirmed by Western blot analysis. Heterozygote mice (F3) were intercrossed to generate $FUS^{-/-}$ mice.

Postmortem human tissues

Specimens of spinal cords from five patients with sporadic ALS and seven other neurological disease patients as controls, as well as temporal lobes from three patients with FTLD-TDP and four other neurological disease patients as controls, were obtained by autopsy with informed consent (Supporting Information Table S1). The diagnosis of ALS was confirmed by El Escorial diagnostic criteria as defined by the World Federation of Neurology and with the presence of TDP-43 pathology, as detected by histopathology. For the diagnosis of FTLD-TDP, selective sections were immunostained with antibodies against phosphorylated tau, ubiquitin, phosphorylated TDP-43 and FUS/TLS to select FTLD-TDP (Cairns et al, 2007). All patients with ALS and FTLD-TDP showed no hereditary traits. The collection of tissues and their use in this study was approved by the ethics committee of Nagoya University Graduate School of Medicine, Fukushimura Hospital, Tokyo Metropolitan Institute, and RIKEN. Tissues for RNA analysis were immediately frozen using liquid nitrogen and stored at −80°C until use. For immunofluorescent staining, 6 μm sections were prepared from paraffin-embedded tissues, deparaffinized, microwaved for 20 min in 50 mM citrate buffer (pH 6.0), treated with TNB blocking buffer (PerkinElmer, Boston, MA) and then incubated with primary antibodies. After washing, sections were incubated with Alexa-546-conjugated goat anti-rabbit IgG (1:1000; Invitrogen) and Alexa-488-conjugated goat anti-mouse IgG (1:1000; Invitrogen) for 30 min, mounted with Prolong gold antifade reagent (Invitrogen) and then imaged with a laser confocal microscope (LSM710, Carl Zeiss, Jena, Germany). The position of the nucleus was confirmed by TO-PRO-3 Iodidel (Invitorgen). For immunohistochemistry, sections were deparaffinized and boiled for 20 min in 50 mM citrate buffer (pH 6.0), treated with 3% goat serum/0.5% tween-20/PBS supplemented with Avidin solution (Vector, Avidin/Biotin Blocking kit, #SP-2001), and then incubated with primary antibodies in 3% goat serum/0.5% tween-20/PBS supplemented with Biotin solution (Vector, Avidin/Biotin Blocking kit). After washing, sections were incubated with Biotin-conjugated anti-mouse IgG or anti-rabbit IgG (1:400, Vector) in 0.05%Tween-20/PBS. Signals were visualized with Vectastain ABC kit (Elite, #PK-6100) and Metal Enhanced DAB substrate kit (Thermo Scientific, #34065).

Quantitative RT-PCR

Prior to RNA extraction, cultured cells were harvested and stored in RNAlater (Ambion), and frozen tissue samples were stored in RNAlater ICE (Ambion). Total RNA containing a small RNA fraction was extracted with a *mir*Vana miRNA Isolation Kit (Ambion) according to the manufacturer's instructions, and then treated with DNase (TURBO DNA-free Kit, Ambion) for either 20 min or 1 h depending on whether the source was cultured cells or tissue samples, respectively. U snRNAs were transcribed with specific primers as described previously (Zhang et al, 2008), and RNA levels were quantified with specific primers as described previously (Zhang et al, 2008) using the Syber Green system (Applied Biosystems). The primers we used are listed in Supporting

Information Table S3. All PCR reactions were performed in triplicate. RNA levels in samples were normalized with GAPDH for mRNA, and average of 5S and 5.8S for small RNA.

For more detailed Materials and Methods see the Supporting Information.

Author contributions

HT and KY designed the study; HT, YI, AF and AK performed the experiments; YI, HH, NA, FT, YH, HA, SM and GS obtained the patient autopsy samples and performed neuropathological and clinical diagnosis; HH and SM advised the staining of human sample; YI, NA, FT and GS provided critical inputs for the manuscript; HT analysed the data and KY provided inputs to analysis; HT and KY wrote the manuscript. All authors approved the manuscript.

Acknowledgements

The authors thank Prof. Haruhiko Siomi (Keio University) for a critical reading of manuscript and advice, and the Research Resource Center of RIKEN Brain Science Institute for their technical support with the Mass spectrometric analysis and generating FUS knockout mice. This work was supported by Grants-in-Aid nos. 23111006 and 23110523 (to KY) for Scientific Research on Innovative Areas, Comprehensive Brain Science Network for Scientific Research on Innovative Areas (to SM, HA), Grant-in-Aid no. 23700455 for Young Scientists (B) (to HT), from the Ministry for Education, Culture, and Sports, Science and Technology of Japan; by Grants-in-Aid (to KY, GS, SM) from the Research Committee of CNS Degenerative Diseases, the Ministry of Health, Labor and Welfare of Japan; and by Research Funding for Longevity Sciences (22-14) (to SM) from the National Center for Geriatrics and Gerontology, Japan.

Supporting Information is available at EMBO Molecular Medicine online.

The authors declare that they have no conflict of interest.

References

Andersen PM, Al-Chalabi A (2011) Clinical genetics of amyotrophic lateral sclerosis: what do we really know? Nat Rev Neurol 7: 603-615

Arai T, Hasegawa M, Akiyama H, Ikeda K, Nonaka T, Mori H, Mann D, Tsuchiya K, Yoshida M, Hashizume Y, *et al* (2006) TDP-43 is a component of ubiquitin-positive tau-negative inclusions in frontotemporal lobar degeneration and amyotrophic lateral sclerosis. Biochem Biophys Res Commun 351: 602-611

Ayala YM, De Conti L, Avendano-Vazquez SE, Dhir A, Romano M, D'Ambrogio A, Tollervey J, Ule J, Baralle M, Buratti E, *et al* (2011) TDP-43 regulates its mRNA levels through a negative feedback loop. EMBO J 30: 277-288

Berg MG, Singh LN, Younis I, Liu Q, Pinto AM, Kaida D, Zhang Z, Cho S, Sherrill-Mix S, Wan L *et al* (2012) U1 snRNP determines mRNA length and regulates isoform expression. Cell 150: 53-64

Blauw HM, Barnes CP, van Vught PW, van Rheenen W, Verheul M, Cuppen E, Veldink JH, van den Berg LH (2012) SMN1 gene duplications are associated with sporadic ALS. Neurology 78: 776-780

Bond CS, Fox AH (2009) Paraspeckles: nuclear bodies built on long noncoding RNA. J Cell Biol 186: 637-644

Boulisfane N, Choleza M, Rage F, Neel H, Soret J, Bordonne R (2011) Impaired minor tri-snRNP assembly generates differential splicing defects of U12-type introns in lymphoblasts derived from a type I SMA patient. Hum Mol Genet 20: 641-648

Buratti E, Dork T, Zuccato E, Pagani F, Romano M, Baralle FE (2001) Nuclear factor TDP-43 and SR proteins promote in vitro and in vivo CFTR exon 9 skipping. EMBO J 20: 1774-1784

Burghes AH, Beattie CE (2009) Spinal muscular atrophy: why do low levels of survival motor neuron protein make motor neurons sick? Nat Rev Neurosci 10: 597-609

Cairns NJ, Bigio EH, Mackenzie IR, Neumann M, Lee VM, Hatanpaa KJ, White CL III, Schneider JA, Grinberg LT, Halliday G, *et al* (2007) Neuropathologic diagnostic and nosologic criteria for frontotemporal lobar degeneration: consensus of the Consortium for Frontotemporal Lobar Degeneration. Acta Neuropathol 114: 5-22

Casafont I, Bengoechea R, Tapia O, Berciano MT, Lafarga M (2009) TDP-43 localizes in mRNA transcription and processing sites in mammalian neurons. J Struct Biol 167: 235-241

Chen-Plotkin AS, Lee VM, Trojanowski JQ (2010) TAR DNA-binding protein 43 in neurodegenerative disease. Nat Rev Neurol 6: 211-220

Cooper TA, Wan L, Dreyfuss G (2009) RNA and disease. Cell 136: 777-793

Coovert DD, Le TT, McAndrew PE, Strasswimmer J, Crawford TO, Mendell JR, Coulson SE, Androphy EJ, Prior TW, Burghes AH (1997) The survival motor neuron protein in spinal muscular atrophy. Hum Mol Genet 6: 1205-1214

Corcia P, Camu W, Halimi JM, Vourc'h P, Antar C, Vedrine S, Giraudeau B, de Toffol B, Andres CR (2006) SMN1 gene, but not SMN2, is a risk factor for sporadic ALS. Neurology 67: 1147-1150

D'Ambrogio A, Buratti E, Stuani C, Guarnaccia C, Romano M, Ayala YM, Baralle FE (2009) Functional mapping of the interaction between TDP-43 and hnRNP A2 in vivo. Nucleic Acids Res 37: 4116-4126

Dion PA, Daoud H, Rouleau GA (2009) Genetics of motor neuron disorders: new insights into pathogenic mechanisms. Nat Rev Genet 10: 769-782

Ebert AD, Yu J, Rose FF, Jr, Mattis VB, Lorson CL, Thomson JA, Svendsen CN (2009) Induced pluripotent stem cells from a spinal muscular atrophy patient. Nature 457: 277-280

Fiesel FC, Voigt A, Weber SS, Van den Haute C, Waldenmaier A, Gorner K, Walter M, Anderson ML, Kern JV, Rasse TM, *et al* (2010) Knockdown of transactive response DNA-binding protein (TDP-43) downregulates histone deacetylase 6. EMBO J 29: 209-221

Gabanella F, Butchbach ME, Saieva L, Carissimi C, Burghes AH, Pellizzoni L (2007) Ribonucleoprotein assembly defects correlate with spinal muscular atrophy severity and preferentially affect a subset of spliceosomal snRNPs. PLoS One 2: e921

Giesemann T, Rathke-Hartlieb S, Rothkegel M, Bartsch JW, Buchmeier S, Jockusch BM, Jockusch H (1999) A role for polyproline motifs in the spinal muscular atrophy protein SMN. Profilins bind to and colocalize with smn in nuclear gems. J Biol Chem 274: 37908-37914

Huang J, Furuya A, Furuichi T (2007) Very-KIND, a KIND domain containing RasGEF, controls dendrite growth by linking Ras small GTPases and MAP2. J Cell Biol 179: 539-552

Kariya S, Re DB, Jacquier A, Nelson K, Przedborski S, Monani UR (2012) Mutant superoxide dismutase 1 (SOD1), a cause of amyotrophic lateral sclerosis, disrupts the recruitment of SMN, the spinal muscular atrophy protein to nuclear Cajal bodies. Hum Mol Genet 21: 3421-3434

Kolb SJ, Battle DJ, Dreyfuss G (2007) Molecular functions of the SMN complex. J Child Neurol 22: 990-994

Kumaran RI, Thakar R, Spector DL (2008) Chromatin dynamics and gene positioning. Cell 132: 929-934

Lagier-Tourenne C, Cleveland DW (2009) Rethinking ALS: the FUS about TDP-43. Cell 136: 1001-1004

Lee EB, Lee VM, Trojanowski JQ (2012) Gains or losses: molecular mechanisms of TDP43-mediated neurodegeneration. Nat Rev Neurosci 13: 38-50

Lemmens R, Moore MJ, Al-Chalabi A, Brown RH, Jr, Robberecht W (2010) RNA metabolism and the pathogenesis of motor neuron diseases. Trends Neurosci 33: 249-258

Mao YS, Zhang B, Spector DL (2011) Biogenesis and function of nuclear bodies. Trends Genet 27: 295-306

Neumann M, Sampathu DM, Kwong LK, Truax AC, Micsenyi MC, Chou TT, Bruce J, Schuck T, Grossman M, Clark CM, *et al* (2006) Ubiquitinated TDP-43 in frontotemporal lobar degeneration and amyotrophic lateral sclerosis. Science 314: 130-133

Okuda T, Hattori H, Takeuchi S, Shimizu J, Ueda H, Palvimo JJ, Kanazawa I, Kawano H, Nakagawa M, Okazawa H (2003) PQBP-1 transgenic mice show a late-onset motor neuron disease-like phenotype. Hum Mol Genet 12: 711-725

Pellizzoni L, Yong J, Dreyfuss G (2002) Essential role for the SMN complex in the specificity of snRNP assembly. Science 298: 1775-1779

Polymenidou M, Lagier-Tourenne C, Hutt KR, Huelga SC, Moran J, Liang TY, Ling SC, Sun E, Wancewicz E, Mazur C, *et al* (2011) Long pre-mRNA depletion and RNA missplicing contribute to neuronal vulnerability from loss of TDP-43. Nat Neurosci 14: 459-468

Rabin SJ, Kim JM, Baughn M, Libby RT, Kim YJ, Fan Y, La Spada A, Stone B, Ravits J (2010) Sporadic ALS has compartment-specific aberrant exon splicing and altered cell-matrix adhesion biology. Hum Mol Genet 19: 313-328

Sephton CF, Cenik C, Kucukural A, Dammer EB, Cenik B, Han Y, Dewey CM, Roth FP, Herz J, Peng J, *et al* (2011) Identification of neuronal RNA targets of TDP-43-containing ribonucleoprotein complexes. J Biol Chem 286: 1204-1215

Shan X, Chiang PM, Price DL, Wong PC (2010) Altered distributions of Gemini of coiled bodies and mitochondria in motor neurons of TDP-43 transgenic mice. Proc Natl Acad Sci USA 107: 16325-16330

Talbot K, Davies KE (2008) Is good housekeeping the key to motor neuron survival? Cell 133: 572-574

Tollervey JR, Curk T, Rogelj B, Briese M, Cereda M, Kayikci M, Konig J, Hortobagyi T, Nishimura AL, Zupunski V, *et al* (2011) Characterizing the RNA targets and position-dependent splicing regulation by TDP-43. Nat Neurosci 14: 452-458

Tripsianes K, Madl T, Machyna M, Fessas D, Englbrecht C, Fischer U, Neugebauer KM, Sattler M (2011) Structural basis for dimethylarginine recognition by the Tudor domains of human SMN and SPF30 proteins. Nat Struct Mol Biol 18: 1414-1420

Ule J (2008) Ribonucleoprotein complexes in neurologic diseases. Curr Opin Neurobiol 18: 516-523

Veldink JH, Kalmijn S, Van der Hout AH, Lemmink HH, Groeneveld GJ, Lummen C, Scheffer H, Wokke JH, Van den Berg LH (2005) SMN genotypes producing less SMN protein increase susceptibility to and severity of sporadic ALS. Neurology 65: 820-825

Veldink JH, van den Berg LH, Cobben JM, Stulp RP, De Jong JM, Vogels OJ, Baas F, Wokke JH, Scheffer H (2001) Homozygous deletion of the survival motor neuron 2 gene is a prognostic factor in sporadic ALS. Neurology 56: 749-752

Wahl MC, Will CL, Luhrmann R (2009) The spliceosome: design principles of a dynamic RNP machine. Cell 136: 701-718

Wan L, Battle DJ, Yong J, Gubitz AK, Kolb SJ, Wang J, Dreyfuss G (2005) The survival of motor neurons protein determines the capacity for snRNP assembly: biochemical deficiency in spinal muscular atrophy. Mol Cell Biol 25: 5543-5551

Wang IF, Reddy NM, Shen CK (2002) Higher order arrangement of the eukaryotic nuclear bodies. Proc Natl Acad Sci USA 99: 13583-13588

Waragai M, Junn E, Kajikawa M, Takeuchi S, Kanazawa I, Shibata M, Mouradian MM, Okazawa H (2000) PQBP-1/Npw38, a nuclear protein binding to the polyglutamine tract, interacts with U5-15kD/dim1p via the carboxyl-terminal domain. Biochem Biophys Res Commun 273: 592-595

Wu CH, Fallini C, Ticozzi N, Keagle PJ, Sapp PC, Piotrowska K, Lowe P, Koppers M, McKenna-Yasek D, Baron DM, *et al* (2012) Mutations in the profilin 1 gene cause familial amyotrophic lateral sclerosis. Nature 488: 499-503

Xiao S, Sanelli T, Dib S, Sheps D, Findlater J, Bilbao J, Keith J, Zinman L, Rogaeva E, Robertson J (2011) RNA targets of TDP-43 identified by UV-CLIP are deregulated in ALS. Mol Cell Neurosci 47: 167-180

Yamazaki T, Chen S, Yu Y, Yan B, Haertlein TC, Carrasco MA, Tapia JC, Zhai B, Das R, Lalancette-Hebert M, *et al* (2012) FUS-SMN protein interactions link the motor neuron diseases ALS and SMA. Cell Rep 2: 799-806

Zhang Z, Lotti F, Dittmar K, Younis I, Wan L, Kasim M, Dreyfuss G (2008) SMN deficiency causes tissue-specific perturbations in the repertoire of snRNAs and widespread defects in splicing. Cell 133: 585-600

RESEARCH PAPER

Neck weakness is a potent prognostic factor in sporadic amyotrophic lateral sclerosis patients

Ryoichi Nakamura,[1] Naoki Atsuta,[1] Hazuki Watanabe,[1] Akihiro Hirakawa,[2] Hirohisa Watanabe,[1] Mizuki Ito,[1] Jo Senda,[1] Masahisa Katsuno,[1] Fumiaki Tanaka,[3] Yuishin Izumi,[4] Mitsuya Morita,[5] Kotaro Ogaki,[6] Akira Taniguchi,[7] Ikuko Aiba,[8] Koichi Mizoguchi,[9] Koichi Okamoto,[10] Kazuko Hasegawa,[11] Masashi Aoki,[12] Akihiro Kawata,[13] Koji Abe,[14] Masaya Oda,[15] Masaaki Konagaya,[16] Takashi Imai,[17] Masanori Nakagawa,[18] Shoji Tsuji,[19] Ryuji Kaji,[4] Imaharu Nakano,[5] Gen Sobue[1]

▶ Additional material is published online only. To view please visit the journal online (http://dx.doi.org/10.1136/jnnp-2013-306020).

For numbered affiliations see end of article.

Correspondence to
Professor Gen Sobue, Department of Neurology, Nagoya University Graduate School of Medicine, 65 Tsurumai-cho, Showa-ku, Nagoya 466–8550 Japan; sobueg@med.nagoya-u.ac.jp

RN and NA contributed equally.

Received 3 June 2013
Revised 17 July 2013
Accepted 18 July 2013
Published Online First 9 August 2013

ABSTRACT

Objective To clarify the emergence of muscle weakness in regions of the body that affect survival, and deterioration in activities of daily living (ADL) in amyotrophic lateral sclerosis (ALS) patients.

Methods We conducted a multicentre-based prospective cohort study of patients with ALS. We enrolled 401 sporadic patients with ALS. Death or the introduction of invasive ventilation was defined as the primary endpoint, and the time to five clinical markers of ADL deterioration associated with bulbar paralysis or limb weakness were defined as ADL milestones. Muscle weakness was assessed in the neck flexor muscles; the bilateral abductors of the shoulders; the bilateral wrist extensor muscles; the bilateral flexor muscles of the hips; and the bilateral ankle dorsiflexion muscles. We performed Cox proportional hazards regression analyses for the primary endpoint and the five ADL milestones, adjusting for known covariate prognostic factors for ALS.

Results The Medical Research Council (MRC) score for the neck flexors was the most significant prognostic factor for the primary endpoint (HR 0.74, p<0.001), *loss of speech* (HR 0.66, p<0.001), and *loss of swallowing function* (HR 0.73, p<0.001), and was one of the significant prognostic factors for *loss of upper limb function*, *difficulty turning in bed*, and *loss of walking ability* (p=0.001, 0.002, and 0.008, respectively). The MRC score for the neck flexors was also a significant prognostic factor for covariates of the previously reported prognostic factors.

Conclusions Neck weakness is an independent prognostic factor for survival and deterioration in ADL in Patients with ALS.

INTRODUCTION

Amyotrophic lateral sclerosis (ALS) is an adult-onset neurodegenerative disease characterised by progressive upper and lower motor neuron loss, which leads to limb and bulbar paralysis and respiratory failure.[1] Symptoms develop at a progressive rate, and the median survival time from disease onset is 2–4 years.[2–4] However, patients with ALS show extensive variability in clinical courses, with durations ranging from a few months to more than 10 years. Furthermore, major symptoms that differentially affect activities of daily living (ADL) and prognosis also show variability among patients with different disease forms.[5] A better understanding of the factors influencing deterioration in ADL and prognosis would help physicians and patients determine whether and when to introduce non-invasive positive pressure ventilation, tube feeding, tracheostomy and artificial ventilation, and would lead to effective stratification strategies in clinical trials. Several studies have shown that age,[6–10] bulbar symptom onset,[6 7] respiratory function,[3 8 11 12] time from symptom onset to diagnosis,[2 6 10 13 14] functional score[2 14] and rate of disease progression[2 15–17] are predictors of survival. Muscle weakness in particular regions of the body affect the prognosis of ALS, although it has not been sufficiently determined which regions are most predictive.[18] To investigate the longitudinal course of patients with ALS and clarify the emergence of muscle weakness, which affects deterioration in ADL and ALS prognosis, we conducted a prospective, multicentre study.

METHODS

Patient registry and follow-up system

We constructed a multicentre registration and follow-up system called the Japanese Consortium for Amyotrophic Lateral Sclerosis research (JaCALS), which consists of 21 neurology facilities in Japan. Patients with ALS diagnosed in these facilities were consecutively registered with written informed consent. The ethics committees of all the participating institutions approved the study. Full clinical examinations were conducted at registration by neurologists in each of the respective institutions. Muscle strength was manually tested and scored with the scale of the Medical Research Council (six points, range: 0–5)[19] in nine muscle groups as follows: neck flexors; bilateral abductors of shoulders as representatives of proximal upper extremity muscles; wrist extensors muscles as representatives of distal upper extremity muscles; bilateral flexors of hips as representatives of proximal lower extremity muscles; and ankle dorsiflexion muscles as representatives of distal lower extremity muscles. All manual muscle testing was performed with standard positioning and procedures by certified neurologists.[20] The MRC score of the neck

To cite: Nakamura R, Atsuta N, Watanabe H, *et al. J Neurol Neurosurg Psychiatry* 2013;**84**: 1365–1371.

flexors was determined with the patient in the supine position. We confirmed the inter-rater reliability of the manual muscle testing method employed in this study using 23 patients with neuromuscular disease. The values of the kappa statistics of each muscle ranged from 0.65 to 0.93. To standardise the procedures and the examinations, the three organising doctors (NA, RN, HaW) visited each participating facility and ascertained the evaluation methods for this study.

Disease onset was defined as when the patients became initially aware of muscle weakness or impairment of swallowing, speech, or respiration. We enrolled patients who fulfilled the revised El Escorial criteria.[21] The diagnostic accuracy of the enrolled patients was then assessed by members of the steering committee of the JaCALS. Included patients were then followed-up with telephone surveys conducted by clinical research coordinators (CRC) or with examinations by neurologists every 3 months, and the degree of deterioration in ADL was determined at each time point. We employed the Japanese version of the ALSFRS-R as a scale for ADL, which was validated by Ohashi *et al*, using a telephone survey system.[22] We confirmed the reliability of the telephone survey system for the Japanese version of the ALSFRS-R previously,[23] and the English version of the telephone survey system has been confirmed in several previous studies.[24–26] Prior to the study, we informed and trained the CRCs of the study plan, procedures for the telephone survey, ethical issues relevant to the study, and requisite considerations for patients with ALS and caregivers, and then provided them with a general knowledge of ALS.

We defined a primary endpoint and ADL milestones in the disease course of the patients with ALS and determined their occurrence by telephone survey or examinations by neurologists. The introduction of tracheostomy positive pressure ventilation (TPPV) or death of the patient was defined as the primary endpoint, and TPPV-free survival was defined as survival. *Loss of speech function*, *loss of swallowing function*, *loss of upper limb function*, *difficulty turning in bed*, and *loss of walking ability* were set as ADL milestones. The time at which each ADL milestone occurred was defined as follows: *loss of speech function* was determined to have occurred when non-vocal communication became needed; *loss of swallowing function* was determined to have occurred when parenteral or enteral feeding became needed exclusively; *loss of upper limb function* occurred when the patient needed to be fed and became unable to grip a pen; *difficulty turning in bed* occurred when the patient became unable to turn in bed alone; *loss of walking ability* occurred when the patient became unable to walk without assistance.

Patients

A total of 520 patients with ALS were initially registered in the JaCALS from January 2006 to June 2011. We excluded 26 patients with known gene mutations: 17 patients with SOD-1 mutations, two patients with TDP-43 mutations, two patients with FUS/TLS mutations, three patients with angiogenin mutations, and two patients with C9ORF72 repeat expansions. We also excluded 13 patients with family histories of ALS and 40 patients who were categorised as clinically possible or suspected according to the revised El Escorial criteria. An additional 20 patients for whom we could not obtain follow-up information to their refusal to participate in the telephone survey were also excluded. Twenty patients were excluded due to invalid data. The study finally included 401 sporadic patients with ALS diagnosed as clinically definite, probable, or probable laboratory-supported. Of these, 382 patients were followed for more than a year or died within a year of registration, and 19 patients were censored within a year from registration. Eleven patients declined the telephone survey during the course of the study, and we lost contact with eight patients during the survey.

Statistical analysis

The clinical data of the registered patients were anonymised in each participating facility of the JaCALS and assigned unique patient numbers. The data were then sent to the clinical data centre located at the Nagoya University Graduate School of Medicine and inputted into the JaCALS database.

We performed Cox proportional hazards regression analyses for the time of registration to the primary endpoint or onset of each ADL milestone to evaluate the impact of muscle weakness on the time to the primary endpoint and each decline in ADL. Specifically, for the primary endpoint and each ADL, we evaluated the HR for the MRC scores in nine muscle groups (ie, neck flexors, left and right abductors of shoulders, wrist extensor muscles, flexors of hips and ankle dorsiflexion muscles) at registration, identifying the muscles groups associated with the primary endpoint and five common ADL milestones. Additionally, we examined the HR for each muscle group after adjusting for known prognostic factors as follows: age at registration,[6–10] gender (male vs female),[6 27] disease duration,[2 6 10 13 14] percent vital capacity (%VC),[3 8 11 12] ALSFRS-R score,[14] riluzole use (yes vs no),[28] bulbar symptom,[6 7] and classification according to the revised El Escorial criteria (definite vs probable or probable laboratory-supported).[7 8 10 14] We compared the time from registration to the primary endpoint or each of the previously defined ADL milestones in the patients divided by their degree of muscle weakness using the Kaplan–Meier method. The log-rank test was used to test the null hypothesis that all the Kaplan–Meier curves were equal. A two-sided $p<0.05$ was considered statistically significant. All statistical analyses were conducted using the PASW V.18.0 program (SPSS Inc, Chicago, Illinois, USA).

RESULTS

Demographic characteristics of the registered patients

The patient sample comprised 244 men and 157 women. The median age at disease onset was 62.2 years (IQR: 53.5–68.5 years), and the mean follow-up period was 2.1±1.5 years. The follow-up rate at 1 year after registration was 95.3%. As initial symptoms, 47.4% of the patients showed upper limb weakness, 31.4% lower limb weakness, 22.9% dysarthria, 5.5% dysphagia and 2.0% cervical weakness. At registration, the median score on the ALSFRS-R was 38 (IQR: 32–42). (see online supplementary table S1).

Identification of weakened muscle groups that affect survival and progression to the ADL milestone

Cox proportional hazard regression analyses for the primary endpoint and the ADL milestones

Table 1 shows the results of Cox proportional hazard regression analyses for the primary endpoint and the five ADL milestones, including the MRC scores of the nine muscle groups. The MRC score for the neck flexors was the most significant negative prognostic factor for the primary endpoint, *loss of speech*, and *loss of swallowing function* (HR 0.74, $p<0.001$, HR 0.66, $p<0.001$, HR 0.73, $p<0.001$, respectively). For the *loss of upper limb function*, *difficulty turning in bed* and *loss of walking ability*, the MRC score for the neck flexors was a significant negative prognostic factor (HR 0.77, $p=0.001$, HR 0.77, $p=0.002$, and HR 0.80, $p=0.008$, respectively). Whereas, the MRC score for the left wrist extensors was a significant positive prognostic factor for the primary endpoint and each ADL milestone except for *difficulty turning in bed*.

Table 1 Multivariate Cox regression analyses for the primary endpoint and each activity of daily living milestone using the MRC score of each muscle group at registration

	Primary endpoint		Loss of speech		Loss of swallowing function		Loss of upper limb function		Difficulty turning in bed		Loss of walking ability	
Muscle group	HR (95% CI)	p Value	HR (95% CI)	p Value	HR (95% CI)	p Value	HR (95% CI)	p Value	HR (95% CI)	p Value	HR (95% CI)	p Value
Neck flexors	0.74 (0.65to 0.86)	<0.001	0.66 (0.56 to 0.76)	<0.001	0.73 (0.63 to 0.85)	<0.001	0.77 (0.66 to 0.89)	0.001	0.77 (0.66 to 0.91)	0.002	0.80 (0.67 to 0.94)	0.008
Left shoulder abductors	0.87 (0.69 to 1.11)	0.266	0.89 (0.69 to 1.14)	0.363	0.89 (0.71 to 1.12)	0.309	0.62 (0.49 to 0.79)	<0.001	0.72 (0.56 to 0.93)	0.012	0.75 (0.57 to 1.00)	0.049
Right shoulder abductors	0.98 (0.77 to 1.25)	0.890	1.11 (0.87 to 1.43)	0.399	1.02 (0.81 to 1.29)	0.867	1.19 (0.94 to 1.50)	0.159	1.08 (0.85 to 1.39)	0.529	0.99 (0.75 to 1.30)	0.917
Left wrist extensors	1.29 (1.04 to 1.59)	0.018	1.28 (1.03 to 1.59)	0.026	1.24 (1.02 to 1.51)	0.034	1.42 (1.14 to 1.77)	0.002	1.24 (1.00 to 1.55)	0.054	1.39 (1.08 to 1.79)	0.010
Right wrist extensors	0.90 (0.74 to 1.08)	0.254	0.88 (0.73 to 1.07)	0.193	0.92 (0.77 to 1.11)	0.380	0.73 (0.60 to 0.88)	0.001	0.80 (0.66 to 0.98)	0.029	0.98 (0.79 to 1.22)	0.884
Left hip flexors	0.99 (0.72 to 1.36)	0.964	0.96 (0.73 to 1.28)	0.791	0.85 (0.62 to 1.15)	0.284	0.74 (0.55 to 0.99)	0.040	0.77 (0.56 to 1.06)	0.115	0.90 (0.61 to 1.32)	0.585
Right hip flexors	0.96 (0.69 to 1.34)	0.830	0.95 (0.70 to 1.28)	0.719	1.09 (0.79 to 1.50)	0.613	1.18 (0.87 to 1.62)	0.290	1.18 (0.84 to 1.66)	0.331	1.06 (0.69 to 1.64)	0.788
Left ankle extensors	1.14 (0.93 to 1.40)	0.214	1.13 (0.94 to 1.34)	0.185	1.14 (0.95 to 1.37)	0.166	1.26 (1.04 to 1.52)	0.021	1.09 (0.91 to 1.30)	0.367	0.93 (0.71 to 1.21)	0.583
Right ankle extensors	0.94 (0.76 to 1.15)	0.530	0.95 (0.79 to 1.14)	0.564	0.94 (0.77 to 1.14)	0.539	0.85 (0.70 to 1.04)	0.125	0.81 (0.68 to 0.97)	0.023	0.72 (0.57 to 0.91)	0.007

According to table 1, the MRC score for the neck flexors was commonly identified as a possible prognostic factor for the primary endpoint and the five ADL milestones. We further examined its impact after adjusting for the other established or potential risk factors, that is, age at registration, gender, disease duration from onset to registration, percent vital capacity (% VC) at registration, ALSFRS-R score at registration, classification according to revised El Escorial criteria, riluzole use and bulbar symptom at registration (table 2). As seen in table 2, the MRC score for the neck flexors was an independent and significant prognostic factor for the primary endpoint, *loss of speech*, *loss of swallowing*, *loss of upper-limb function* and *difficulty turning in bed* in patients with ALS except for *loss of walking ability.* ($p<0.001$, $p=0.001$, $p=0.003$, $p<0.001$, $p=0.027$, respectively). At registration, there were moderate and significant correlations between the MRC score for the neck flexors and the % VC or the ALSFRS-R score. Pearson's correlation coefficients were 0.367 ($p<0.001$) and 0.496 ($p<0.001$), respectively.

Differences in survival time and time to ADL milestones in patients in terms of the MRC score grade for the neck flexors

We divided the registered patients into four categories according to their MRC score for the neck flexors (ie, 5, 4, 3 and ≤2). Figure 1 shows the Kaplan–Meier curves for the four categories for the primary endpoint and each ADL milestone. All the differences between the curves were significant according to a log-rank test ($p<0.001$).

DISCUSSION

In a prospective and multicentre cohort study, we identified that weakness of the neck flexors is a potent factor for the prediction of survival and for the deterioration of ADL, such as speech, swallowing, upper limb function, turning in bed, and walking, in sporadic patients with ALS.

The neck flexors consist of the sternocleidomastoid muscle (SCM), the platysma muscle, hyoid muscle, longus capitis muscle, longus colli and scalenus. These muscles are innervated by motor neurons in the cervical cord (C1–8) and accessory nerve nuclei,[29 30] primarily the C2–4 segments. By contrast, respiratory muscles consist of the diaphragm and the internal and external intercostals muscles, which are innervated by motor neurons of the upper cervical cord (C3–5) and thoracic cord (Th1–Th12), respectively.[30] Thus, the muscles for neck flexion and those for respiration partially share spinal segments of the motor neuron column for their motor innervations. Furthermore, significant correlations are present between compound muscle action potentials of the SCM and those of the diaphragm in patients with ALS,[31] suggesting that neck muscle weakness is correlated with weakness of the diaphragm to some extent in ALS. Because the main cause of death in patients with ALS is respiratory insufficiency, it is reasonable that neck flexor weakness was associated with respiratory impairments and, eventually, survival time. The motor response amplitude of the phrenic nerve motor neurons which are located in the C3–5 segments has been shown to be a significant prognostic factor for survival in patients with ALS.[32] This supports our findings.

Why then is weakness of the neck flexors a determinant factor for the deterioration of ADL for speech, swallowing, upper limb function, truncal turning and walking ability? Recently, some studies have suggested that the degeneration of motor neurons is initially a focal process in ALS that later spreads contiguously throughout the three-dimensional anatomy of connected or neighbouring neurons.[33–36] Dysfunction of speech and swallowing involves the impairment of motor

Table 2 Multivariate Cox regression analyses with the adjustments of the covariates that we selected for the primary endpoint and each activity of daily living milestone using known predictive factors

	Primary endpoint		Loss of speech		Loss of swallowing function		Loss of upper limb function		Difficulty turning in bed		Loss of walking ability	
	HR (95% CI)	p Value	HR (95% CI)	p Value	HR (95% CI)	p Value	HR (95% CI)	p Value	HR (95% CI)	p Value	HR (95% CI)	p Value
MRC score of neck flexors at registration	0.72 (0.62 to 0.83)	<0.001	0.78 (0.67 to 0.90)	0.001	0.80 (0.69 to 0.93)	0.003	0.76 (0.65 to 0.88)	<0.001	0.83 (0.70 to 0.98)	0.027	0.95 (0.79 to 1.15)	0.601
Age at registration (years)	1.03 (1.02 to 1.04)	<0.001	1.02 (1.01 to 1.03)	0.002	1.03 (1.01 to 1.04)	<0.001	1.01 (0.99 to 1.02)	0.264	1.01 (0.99 to 1.02)	0.265	1.00 (0.98 to 1.01)	0.890
Gender (male vs female)	1.14 (0.85 to 1.52)	0.381	0.85 (0.65 to 1.12)	0.247	1.13 (0.85 to 1.49)	0.398	1.27 (0.97 to 1.68)	0.088	1.01 (0.76 to 1.33)	0.947	0.85 (0.61 to 1.17)	0.309
Duration from onset to registration (years)	0.64 (0.57 to 0.72)	<0.001	0.72 (0.64 to 0.80)	<0.001	0.69 (0.62 to 0.77)	<0.001	0.82 (0.75 to 0.9)	<0.001	0.74 (0.65 to 0.85)	<0.001	0.75 (0.66 to 0.87)	<0.001
%VC at registration	0.98 (0.98 to 0.99)	<0.001	0.98 (0.97 to 0.99)	<0.001	0.98 (0.98 to 0.99)	<0.001	0.99 (0.98 to 1.00)	0.001	0.99 (0.99 to 1.00)	0.007	1.00 (0.99 to 1.00)	0.491
ALSFRS-R at registration	0.97 (0.94 to 0.99)	0.008	0.99 (0.97 to 1.02)	0.483	0.96 (0.93 to 0.98)	0.001	0.96 (0.94 to 0.98)	0.001	0.89 (0.86 to 0.92)	<0.001	0.91 (0.88 to 0.94)	<0.001
El Escorial criteria (probable or probable laboratory-supported)	0.72 (0.53 to 0.99)	0.043	0.61 (0.45 to 0.82)	0.001	0.76 (0.56 to 1.04)	0.087	0.67 (0.50 to 0.90)	0.007	0.71 (0.52 to 0.97)	0.031	0.63 (0.44 to 0.88)	0.008
Riluzole administration	1.02 (0.75 to 1.37)	0.916	1.09 (0.82 to 1.44)	0.551	0.97 (0.73 to 1.29)	0.843	0.95 (0.72 to 1.25)	0.694	0.84 (0.63 to 1.13)	0.258	0.94 (0.68 to 1.31)	0.721
Bulbar symptom at registration	0.91 (0.67 to 1.22)	0.524	2.04 (1.52 to 2.73)	<0.001	1.41 (1.06 to 1.86)	0.018	0.68 (0.50 to 0.93)	0.015	0.63 (0.47 to 0.84)	0.002	0.68 (0.49 to 0.96)	0.028

%VC, percent vital capacity; ALSFRS-R, revised amyotrophic lateral sclerosis functional rating scale.

neurons relayed via the glossopharyngeal, vagus, accessory and hypoglossal nerves to the medulla oblongata.[30] The medulla oblongata and cervical cord motor neurons innervating the neck flexion muscles are anatomically different in their three-dimensional layering, while these two groups of neurons are rather contiguously located. Thus, it may be speculated that if the contiguous spreading of motor neuron degeneration occurs according to the local spreading hypothesis, neck flexion impairment may eventually affect speech and swallowing functions. Furthermore, motor neurons for the neck flexion muscles, which are located in the C1–8 segments,[29 30] are also contiguous or overlapping with those for the upper limb muscles in the C5–Th1 segments, particularly the proximal upper limb muscles.[29 30] Neck flexion and upper limb function may be correlated with disease progression through the local spreading view of motor neuron degeneration. Truncal turning and walking require not only lower limb muscle activities but also power in a broad area of the chest, abdominal and back muscles, which are innervated by the cervical to lumbar cord.[37–39] Therefore, propagation of weakness from the cervical and lumbar areas may affect truncal turning or walking. We need, however, further investigations to demonstrate the underlying mechanisms of the correlation between the neck muscles and other muscles of the body that together determine ADL.

In this study, the MRC score for the left wrist extensors shows a positive prognostic factor for the primary endpoint and some ADL milestones, the reason for which might be that the weakness of the distal muscle in the non-dominant arm was least relevant to survival, or ADL declines so that it was shown to be a positive factor in the multivariate analyses.

A number of studies have demonstrated survival curves for patients with ALS and some factors that influence these survival curves.[18] The majority of these studies have found that older age is a strong risk factor for shorter survival in patients with ALS,[6–10] and the onset of bulbar symptoms is associated with a worse prognosis than the onset of spinal symptoms.[6 7] Several studies have found that a longer diagnostic delay correlates with a better prognosis,[2 6 10 13 14] and that a lower %VC or a percent forced vital capacity (%FVC) is correlated with shorter survival for patients with ALS.[3 8 11 12] The progression rate of the ALSFRS-R at the time of diagnosis was also related to ALS prognosis.[17] Neck flexor weakness has not been listed as a prognostic factor for patients with ALS, and most of these studies evaluated survival alone as an endpoint, and did not determine the onset of loss of speech, swallowing, limb and truncal function. In this study, we showed that neck flexor weakness was not only a novel prognostic factor for survival but also a significant prognostic marker for non-survival events related to ADL decline for patients with ALS.

In the course of ALS, patients must make some difficult decisions, including the use of gastrostomy for tube feeding, the use of assisted ventilation, and end-of-life planning, which require the support of the attending physician and a multidisciplinary team. All patients with ALS should be provided with sufficient information concerning these interventions and given sufficient opportunity for the careful consideration of their decision. In the medical, nursing and social care of patients with ALS, simple and robust indicators for predicting the status of each patient for several months or a year after diagnosis are necessary for patient management. Medical staff and caregivers need to have a predictor of the patient's status in the near future, including survival prognosis and also estimates for the loss of speech, swallowing, limb and truncal function. Our findings may contribute to such prediction.

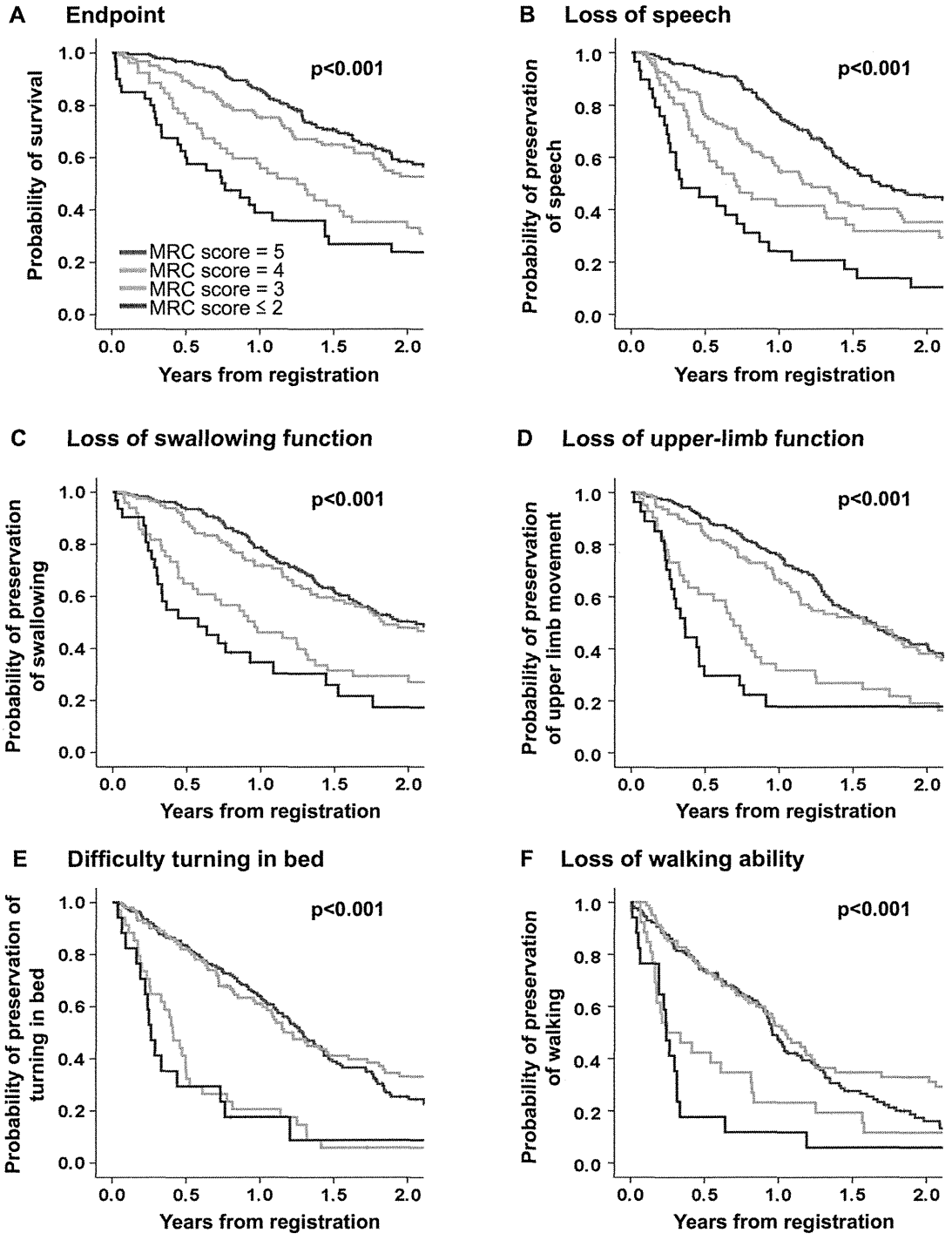

Figure 1 Kaplan–Meier curves according to the MRC score for the neck flexors. The Kaplan–Meier curves for the primary endpoint and each activity of daily living milestone among four categories divided according to the MRC score for the neck flexors were compared by the log-rank test. Curves are shown for the MRC score 5 (blue), the MRC score 4 (green), the MRC score 3 (orange), and the MRC score ≤2 (purple) groups. All the differences of the curves were significant (p<0.001).

The course of ALS is highly variable between patients,[5] which is one of the major factors limiting the power of ALS clinical trials.[40 41] Therefore, robust stratification factors that could divide ALS patient groups depending upon prognosis are needed for designing trials. Compared with known prognostic factors for patients with ALS, such as age, duration from onset to registration, ALSFRS-R at registration, and presence of bulbar symptom, weakness of the neck flexors was a potent and independent prognostic factor. Thus, the MRC score for the neck flexors might be used for stratification factor in a future clinical trial.

Neck extensor muscle weakness with head drop as an early symptom has been reported in a few patients with ALS.[42 43] However, Katz *et al*[44] wrote that neck flexor weakness is typically observed. We assert that neck flexor weakness is commonly observed in patients with ALS, and is useful for the prediction of prognosis.

The limitations of this study are as follows: registered patients were followed-up by telephone survey, and we did not examine longitudinal changes in the strength of multiple muscles. As we demonstrated, the relationship between the involved muscle groups and survival prognosis and estimates of ADL deterioration would offer insights into the modalities of progression in patients with ALS. However, to examine the pattern of spread more precisely, a cohort study that observes longitudinal changes in the strength of muscle groups and extensions of muscle weakness will be required.

This study analysed a multicentre cohort of patients with ALS in a single nation, Japan. Although the clinical profiles of ALS are broadly similar among countries in previous reports, the outcome of our study would be better confirmed in cohorts of patients with ALS in multiple countries.

In conclusion, we showed that neck weakness is an independent prognostic factor for survival and deterioration in ADL in patients with ALS. We hope that our report will be helpful for clinicians who want to provide medical, social and nursing care to patients with ALS with proper timing, and to researchers as they plan clinical trials for ALS.

Author affiliations
[1]Department of Neurology, Nagoya University Graduate School of Medicine, Nagoya, Japan
[2]Biostatistics Section, Center for Advanced Medicine and Clinical Research, Nagoya University Graduate School of Medicine, Nagoya, Japan
[3]Department of Neurology, Yokohama City University Graduate School of Medicine, Yokohama, Japan
[4]Department of Clinical Neuroscience, Institute of Health Biosciences, University of Tokushima Graduate School, Tokushima, Japan
[5]Division of Neurology, Department of Internal Medicine, Jichi Medical University, Tochigi, Japan
[6]Department of Neurology, Juntendo University School of Medicine, Tokyo, Japan
[7]Department of Neurology, Mie University Graduate School of Medicine, Tsu, Japan
[8]Department of Neurology, National Hospital Organization Higashinagoya National Hospital, Nagoya, Japan
[9]Department of Neurology, Shizuoka Institute of Epilepsy and Neurological Disorders, Shizuoka, Japan
[10]Department of Neurology, Gunma University Graduate School of Medicine, Gunma, Japan
[11]Division of Neurology, National Hospital Organization, Sagamihara National Hospital, Sagamihara, Japan
[12]Department of Neurology, Tohoku University School of Medicine, Sendai, Japan
[13]Department of Neurology, Tokyo Metropolitan Neurological Hospital, Tokyo, Japan
[14]Department of Neurology, Okayama University Graduate School of Medicine, Okayama, Japan
[15]Department of Neurology, Vihara Hananosato Hospital, Miyoshi, Japan
[16]Department of Neurology, National Hospital Organization, Suzuka National Hospital, Suzuka, Japan
[17]Division of Neurology, National Hospital Organization, Miyagi National Hospital, Miyagi, Japan
[18]Director of North Medical Center, Kyoto Prefectural University of Medicine, Kyoto, Japan
[19]Department of Neurology, Graduate School of Medicine, The University of Tokyo, Tokyo, Japan

Acknowledgements We thank all Patients with ALS who participated in this study. We also thank all participating doctors and staff of JaCALS.

Collaborators JaCALS members included Drs Tatsuhiko Yuasa (Kamagaya General Hospital); Takahiro Kano (Hokkaido University); Hidenao Sasaki (Hokkaido University); Masaaki Kato (Tohoku University); Tomohiko Ishihara (Niigata University); Masatoyo Nishizawa (Niigata University); Masaki Ikeda (Gunma University); Kazumoto Shibuya (Chiba University); Satoshi Kuwabara (Chiba University); Hideaki Hayashi, MD (Tokyo Metropolitan Neurological Hospital); Yuji Takahashi (The University of Tokyo); Hiroyuki Tomiyama (Juntendo University); Nobutaka Hattori (Juntendo University); Hitoshi Aizawa (Tokyo National Hospital); Osamu Kano (Toho University Omori Medical Center); Yasuo Iwasaki (Toho University Omori Medical Center); Takamura Nagasaka (University of Yamanashi); Yoshihisa Takiyama (University of Yamanashi); Motoko Sakai (Suzuka National Hospital); Kensuke Shiga (Kyoto Prefectural University); Hirofumi Yamashita (Kyoto University); Ryosuke Takahashi (Kyoto University); Takuji Fujita (Takumikai Neurology Clinic); Toru Yamashita (Okayama University); Masanori Hiji (Vihara Hananosato Hospital); Yasuhiro Watanabe (Tottori University); Kenji Nakashima (Tottori University); Shintaro Hayashi (Kyushu University); and Jun-ichi Kira (Kyushu University).

Contributors RN: drafting/revising the manuscript, acquisition, analysis and interpretation of the data, statistical analysis, and research project execution; NA: drafting/revising the manuscript, acquisition, analysis and interpretation of the data, statistical analysis, research project execution, and study design and concept; HaW: acquisition and interpretation of the data, and research project execution; AH: manuscript review and critique, analysis and interpretation of the data, and statistical analysis design; HiW and MI: acquisition and interpretation of the data, research project execution, and study design and concept; JS, MKatsu, FT, Yul, KotO, AT, IA, KM, KoiO, KH, AK, KA, MO, MKo, Tal, MNa, and IN: revising the manuscript, and acquisition and interpretation of the data; MM, MA, ST, and RK: revising the manuscript, acquisition and interpretation of the data, and the members of the JaCALS steering committee; GS: research project organisation and execution, drafting/revising the manuscript, interpretation of the data, study design and concept, and the member of the JaCALS steering committee. TY: the member of the JaCALS steering committee; TK, HS, MKato, Tol, MNi, MI, KaS, SK, HH, YuT, HT, NH, HA, OK, Yal, TN, YaT, MS, KeS, HY, RT, TF, TY, MH, YW, KN, SH, and JK: acquisition of the data.

Funding This study was supported by Health and Labour Sciences Research grants (Research on intractable diseases H23-015 and H24-012) and grants-in-Aid for Scientific Research from the Ministry of Education, Culture, Sports, Science and Technology (MEXT) of Japan (grant number 25461277).

Competing interests None.

Ethics approval The ethics committees of all the participating institutions approved the study.

Provenance and peer review Not commissioned; externally peer reviewed.

REFERENCES

1 Rowland LP, Shneider NA. Amyotrophic lateral sclerosis. *N Engl J Med* 2001;344:1688–700.
2 Haverkamp LJ, Appel V, Appel SH. Natural history of amyotrophic lateral sclerosis in a database population. Validation of a scoring system and a model for survival prediction. *Brain* 1995;118:707–19.
3 Ringel SP, Murphy JR, Alderson MK, *et al*. The natural history of amyotrophic lateral sclerosis. *Neurology* 1993;43:1316–22.
4 Norris F, Shepherd R, Denys E, *et al*. Onset, natural history and outcome in idiopathic adult motor neuron disease. *J Neurol Sci* 1993;118:48–55.
5 Chio A, Calvo A, Moglia C, *et al*. Phenotypic heterogeneity of amyotrophic lateral sclerosis: a population based study. *J Neurol Neurosurg Psychiatry* 2011;82:740–6.
6 del Aguila MA, Longstreth WT Jr, McGuire V, *et al*. Prognosis in amyotrophic lateral sclerosis: a population-based study. *Neurology* 2003;60:813–19.
7 Magnus T, Beck M, Giess R, *et al*. Disease progression in amyotrophic lateral sclerosis: predictors of survival. *Muscle Nerve* 2002;25:709–14.
8 Chio A, Mora G, Leone M, *et al*. Early symptom progression rate is related to ALS outcome: a prospective population-based study. *Neurology* 2002;59:99–103.
9 Christensen PB, Hojer-Pedersen E, Jensen NB. Survival of patients with amyotrophic lateral sclerosis in 2 Danish counties. *Neurology* 1990;40:600–4.
10 Millul A, Beghi E, Logroscino G, *et al*. Survival of patients with amyotrophic lateral sclerosis in a population-based registry. *Neuroepidemiology* 2005;25:114–19.
11 Stambler N, Charatan M, Cedarbaum JM. Prognostic indicators of survival in ALS. ALS CNTF Treatment Study Group. *Neurology* 1998;50:66–72.
12 Czaplinski A, Yen AA, Appel SH. Forced vital capacity (FVC) as an indicator of survival and disease progression in an ALS clinic population. *J Neurol Neurosurg Psychiatry* 2006;77:390–2.
13 Czaplinski A, Yen AA, Appel SH. Amyotrophic lateral sclerosis: early predictors of prolonged survival. *J Neurol* 2006;253:1428–36.
14 Kaufmann P, Levy G, Thompson JL, *et al*. The ALSFRSr predicts survival time in an ALS clinic population. *Neurology* 2005;64:38–43.
15 Armon C, Graves MC, Moses D, *et al*. Linear estimates of disease progression predict survival in patients with amyotrophic lateral sclerosis. *Muscle Nerve* 2000;23:874–82.
16 Armon C, Moses D. Linear estimates of rates of disease progression as predictors of survival in patients with ALS entering clinical trials. *J Neurol Sci* 1998;160(Suppl 1): S37–41.
17 Kimura F, Fujimura C, Ishida S, *et al*. Progression rate of ALSFRS-R at time of diagnosis predicts survival time in ALS. *Neurology* 2006;66:265–7.
18 Chio A, Logroscino G, Hardiman O, *et al*. Prognostic factors in ALS: a critical review. *Amyotroph Lateral Scler* 2009;10:310–23.
19 Medical Research Council. *Aids to the examination of the peripheral nervous system*. London: Her Majesty's Stationery Office, 1976.
20 Campbell WW. *Dejong's Neurologic Examination*. Philadelphia, USA: Lippincott Williams & Wilkins, 2005.

21 Brooks BR, Miller RG, Swash M, *et al*. El Escorial revisited: revised criteria for the diagnosis of amyotrophic lateral sclerosis. *Amyotroph Lateral Scler Other Motor Neuron Disord* 2000;1:293–9.
22 Ohashi Y, Tashiro K, Itoyama Y, *et al*. Study of functional rating scale for amyotrophic lateral sclerosis: revised ALSFRS(ALSFRS-R) Japanese version. *No To Shinkei* 2001;53:346–55.
23 Atsuta N, Watanabe H, Ito M, *et al*. Development of a telephone survey system for patients with amyotrophic lateral sclerosis using the ALSFRS-R (Japanese version) and application of this system in a longitudinal multicenter study. *Brain Nerve* 2011;63:491–6.
24 Kasarskis EJ, Dempsey-Hall L, Thompson MM, *et al*. Rating the severity of ALS by caregivers over the telephone using the ALSFRS-R. *Amyotroph Lateral Scler Other Motor Neuron Disord* 2005;6:50–4.
25 Kaufmann P, Levy G, Montes J, *et al*. Excellent inter-rater, intra-rater, and telephone-administered reliability of the ALSFRS-R in a multicenter clinical trial. *Amyotroph Lateral Scler* 2007;8:42–6.
26 Mannino M, Cellura E, Grimaldi G, *et al*. Telephone follow-up for patients with amyotrophic lateral sclerosis. *Eur J Neurol* 2007;14:79–84.
27 Chancellor AM, Slattery JM, Fraser H, *et al*. The prognosis of adult-onset motor neuron disease: a prospective study based on the Scottish Motor Neuron Disease Register. *J Neurol* 1993;240:339–46.
28 Miller RG, Mitchell JD, Moore DH. Riluzole for amyotrophic lateral sclerosis (ALS)/ motor neuron disease (MND). *Cochrane Database Syst Rev* 2012;3:CD001447.
29 Brendler SJ. Human cervical myotomes—functional anatomy studied at operation. *J Neurosurg* 1968;28:105–11.
30 Parent A. *Carpenter's human neuroanatomy*. Quebec, Canada: Williams & Wilkins, 1996.
31 Pinto S, de Carvalho M. Motor responses of the sternocleidomastoid muscle in patients with amyotrophic lateral sclerosis. *Muscle Nerve* 2008;38:1312–17.
32 Pinto S, Pinto A, de Carvalho M. Phrenic nerve studies predict survival in amyotrophic lateral sclerosis. *Clin Neurophysiol* 2012;123:2454–9.
33 Ravits JM, La Spada AR. ALS motor phenotype heterogeneity, focality, and spread: deconstructing motor neuron degeneration. *Neurology* 2009;73:805–11.
34 Fujimura-Kiyono C, Kimura F, Ishida S, *et al*. Onset and spreading patterns of lower motor neuron involvements predict survival in sporadic amyotrophic lateral sclerosis. *J Neurol Neurosurg Psychiatry* 2011;82:1244–9.
35 Kanouchi T, Ohkubo T, Yokota T. Can regional spreading of amyotrophic lateral sclerosis motor symptoms be explained by prion-like propagation? *J Neurol Neurosurg Psychiatry* 2012;83:739–45.
36 Brettschneider J, Tredici KD, Toledo JB, *et al*. Stages of pTDP-43 pathology in amyotrophic lateral sclerosis. *Ann Neurol* Published Online First: 20 May 2013. doi:10.1002/ana.23937.
37 Kavanagh J, Barrett R, Morrison S. The role of the neck and trunk in facilitating head stability during walking. *Exp Brain Res* 2006;172:454–63.
38 Ballesteros ML, Buchthal F, Rosenfalck P. The pattern of muscular activity during the arm swing of natural walking. *Acta Physiol Scand* 1965;63:296–310.
39 Richter RR, VanSant AF, Newton RA. Description of adult rolling movements and hypothesis of developmental sequences. *Phys Ther* 1989;69:63–71.
40 Cudkowicz ME, Katz J, Moore DH, *et al*. Toward more efficient clinical trials for amyotrophic lateral sclerosis. *Amyotroph Lateral Scler* 2010;11:259–65.
41 Sorenson EJ. What is next in ALS clinical trials? *Neurology* 2007;69:719–20.
42 Gourie-Devi M, Nalini A, Sandhya S. Early or late appearance of "dropped head syndrome" in amyotrophic lateral sclerosis. *J Neurol Neurosurg Psychiatry* 2003;74:683–6.
43 Uemura M, Kosaka T, Shimohata T, *et al*. *et al*. Dropped head syndrome in amyotrophic lateral sclerosis. *Amyotroph Lateral Scler Frontotemporal Degeneration* 2013;14:232–3.
44 Katz JS, Wolfe GI, Burns DK, *et al*. Isolated neck extensor myopathy: a common cause of dropped head syndrome. *Neurology* 1996;46:917–21.

JNNP

Neck weakness is a potent prognostic factor in sporadic amyotrophic lateral sclerosis patients

Ryoichi Nakamura, Naoki Atsuta, Hazuki Watanabe, Akihiro Hirakawa, Hirohisa Watanabe, Mizuki Ito, Jo Senda, Masahisa Katsuno, Fumiaki Tanaka, Yuishin Izumi, Mitsuya Morita, Kotaro Ogaki, Akira Taniguchi, Ikuko Aiba, Koichi Mizoguchi, Koichi Okamoto, Kazuko Hasegawa, Masashi Aoki, Akihiro Kawata, Koji Abe, Masaya Oda, Masaaki Konagaya, Takashi Imai, Masanori Nakagawa, Shoji Tsuji, Ryuji Kaji, Imaharu Nakano and Gen Sobue

J Neurol Neurosurg Psychiatry 2013 84: 1365-1371 originally published online August 9, 2013
doi: 10.1136/jnnp-2013-306020

doi:10.1093/brain/awt029 Brain 2013: 136; 1371–1382 | 1371

BRAIN
A JOURNAL OF NEUROLOGY

Loss of TDP-43 causes age-dependent progressive motor neuron degeneration

Yohei Iguchi,[1] Masahisa Katsuno,[1] Jun-ichi Niwa,[2] Shinnosuke Takagi,[1] Shinsuke Ishigaki,[1] Kensuke Ikenaka,[1] Kaori Kawai,[1] Hirohisa Watanabe,[1] Koji Yamanaka,[3,4] Ryosuke Takahashi,[5] Hidemi Misawa,[6] Shoichi Sasaki,[7] Fumiaki Tanaka[1,8] and Gen Sobue[1,4]

1 Department of Neurology, Nagoya University Graduate School of Medicine, Nagoya 466-8550, Japan
2 Stroke Centre, Aichi Medical University, Aichi 480-1195, Japan
3 Laboratory for Motor Neuron Disease, RIKEN Brain Science Institute, Wako, Saitama 351-0198, Japan
4 CREST, Japan Science and Technology Agency, 4-1-8, Honcho, Kawaguchi, Saitama 332-0012, Japan
5 Department of Neurology, Kyoto University Graduate School of Medicine, Kyoto 606-8507, Japan
6 Department of Pharmacology, Keio University Faculty of Pharmacy, Tokyo 105-8512, Japan
7 Department of Neurology, Neurological Institute, Tokyo Women's Medical University, Tokyo 162-8666, Japan
8 Department of Neurology and Stroke Medicine, Yokohama City University Graduate School of Medicine, Yokohama 236-0004, Japan

Correspondence to: Gen Sobue
Showa-ku, Nagoya 466-8550,
Japan
E-mail: sobueg@med.nagoya-u.ac.jp

Amyotrophic lateral sclerosis is a devastating, progressive neurodegenerative disease that affects upper and lower motor neurons. Although several genes are identified as the cause of familial cases, the pathogeneses of sporadic forms, which account for 90% of amyotrophic lateral sclerosis, have not been elucidated. Transactive response DNA-binding protein 43 a nuclear protein regulating RNA processing, redistributes to the cytoplasm and forms aggregates, which are the histopathological hallmark of sporadic amyotrophic lateral sclerosis, in affected motor neurons, suggesting that loss-of-function of transactive response DNA-binding protein 43 is one of the causes of the neurodegeneration. To test this hypothesis, we assessed the effects of knockout of transactive response DNA-binding protein 43 in mouse postnatal motor neurons using Cre/loxp system. These mice developed progressive weight loss and motor impairment around the age of 60 weeks, and exhibited degeneration of large motor axon, grouped atrophy of the skeletal muscle, and denervation in the neuromuscular junction. The spinal motor neurons lacking transactive response DNA-binding protein 43 were not affected for 1 year, but exhibited atrophy at the age of 100 weeks; whereas, extraocular motor neurons, that are essentially resistant in amyotrophic lateral sclerosis, remained preserved even at the age of 100 weeks. Additionally, ultra structural analysis revealed autolysosomes and autophagosomes in the cell bodies and axons of motor neurons of the 100-week-old knockout mice. In summary, the mice in which transactive response DNA-binding protein 43 was knocked-out specifically in postnatal motor neurons exhibited an age-dependent progressive motor dysfunction accompanied by neuropathological alterations, which are common to sporadic amyotrophic lateral sclerosis. These findings suggest that transactive response DNA-binding protein 43 plays an essential role in the long term maintenance of motor neurons and that loss-of-function of this protein seems to contribute to the pathogenesis of amyotrophic lateral sclerosis.

Keywords: transactive response DNA-binding protein 43; amyotrophic lateral sclerosis; axonal degeneration; autophagosome

Abbreviations: ALS = amyotrophic lateral sclerosis; FTLD = frontotemporal lobar degeneration; TDP CKO = motor neuron-specific TDP-43 knockout; TDP hCKO = TDP heterozygous CKO

Received July 20, 2012. Revised December 17, 2012. Accepted December 28, 2012. Advance Access publication February 28, 2013

Introduction

Amyotrophic lateral sclerosis (ALS) is a progressive, fatal neurodegenerative disease that affects upper and lower motor neurons in the brain stem and spinal cord. Although previous studies using animal models of ALS have focused mainly on the toxicity of mutant SOD1, one of the causative genes of familial ALS (ALS1), there are pathophysiological differences between ALS1 and sporadic ALS that accounts for ~90% of ALS. The most striking recent discovery regarding ALS is that transactive response DNA-binding protein 43 (TDP-43) was identified as a major component of ubiquitinated neuronal cytoplasmic inclusions in both sporadic ALS and frontotemporal lobar degeneration (FTLD) (Arai *et al.*, 2006; Neumann *et al.*, 2006). In addition, TDP-43 is a causative gene of familial ALS (ALS10) (Gitcho *et al.*, 2008; Kabashi *et al.*, 2008; Sreedharan *et al.*, 2008; Yokoseki *et al.*, 2008). Taken together, these data suggest that TDP-43 plays a key role in the pathogenesis of sporadic ALS. Although TDP-43 is a nuclear protein, it redistributes to the cytoplasm and forms aggregates in affected neurons of patients with sporadic ALS (Arai *et al.*, 2006; Neumann *et al.*, 2006), suggesting that loss of TDP-43 function underlies sporadic ALS pathogenesis. TDP-43 is known to regulate gene transcription, stability of messenger RNA, and exon splicing through interactions with RNA, heterogeneous nuclear ribonucleoproteins and nuclear bodies (Wang *et al.*, 2004; Ayala *et al.*, 2005; Buratti *et al.*, 2005, 2010; Strong *et al.*, 2007; Polymenidou *et al.*, 2011; Sephton *et al.*, 2011; Tollervey *et al.*, 2011). Knockdown of TDP-43 in neuronal cells inhibits neurite outgrowth and diminishes cell viability (Iguchi *et al.*, 2009), whereas TDP-43 depletion induces apoptosis in HeLa or U2OS cells (Ayala *et al.*, 2008). In addition, *Drosophila* without TDP-43 present deficient locomotive behaviours, reduced life span and anatomical defects at neuromuscular junctions (Feiguin *et al.*, 2009). TDP-43-depleted zebrafish exhibit swimming deficits along with excessive, premature branching and shortened motor axons (Kabashi *et al.*, 2011). Furthermore, TDP-43 knockout mice are embryonic lethal (Kraemer *et al.*, 2010; Sephton *et al.*, 2010; Wu *et al.*, 2010), and postnatal deletion of TDP-43 leads to rapid death with loss of body fat (Chiang *et al.*, 2010). Although these findings indicate that TDP-43 is essential for survival of mice at both embryonic and post-natal stages, the effects of TDP-43 depletion in postnatal mammalian neurons have not been fully elucidated. In the present study, we generated motor neuron-specific TDP-43 knockout (TDP CKO) mice using the Cre/loxP recombination system to investigate the effects of TDP-43 loss on postnatal motor neurons in mice.

Materials and methods

Generation and maintenance of TDP-43 conditional knockout mouse

The targeting construct was designed to insert an Frt-flanked neomycin cassette and a loxP site upstream, and a loxP site downstream of the second exon of the *Tardbp* gene. This construct was electroporated into iTL1 BA1 (C57BL/6 × 129/SvEv) hybrid embryonic stem cells. Correctly targeted embryonic stem cells were injected into recipient blastocysts and chimeric mice were bred with C57BL/6J mice. The resulting En1flox-neo mice were then bred to C57BL/6J mice constitutively expressing Flp recombinase to remove the Frt-flanked neo cassette, generating En1flox offspring. En1flox mutant mice were backcrossed with C57BL/6J mice for at least five generations, and then crossed with VAChT-Cre.Fast mice, which are the most validated mice that specifically express Cre in motor neurons (Misawa *et al.*, 2003). To generate TDP-43 conditional knockout mice, we crossed TDP-43$^{flox/flox}$ mice with TDP-43$^{flox/+}$/VAChT-Cre mice. Finally, we obtained TDP-43$^{flox/flox}$/VAChT-Cre (motor neuron-specific TDP-43 knockout: TDP CKO), TDP-43$^{flox/+}$/VAChT-Cre (TDP heterozygous CKO: TDP hCKO), TDP-43$^{flox/flox}$ and TDP-43$^{flox/+}$ mice. The TDP-43$^{flox/flox}$ mice were then used as control littermates in the present analyses. Mice were kept on a 12-h light/12-h dark cycle, with food and water provided *ad libitum*. All animal experiments were performed in accordance with the National Institutes of Health Guide for the Care and Use of Laboratory Animals and under the approval of the Nagoya University Animal Experiment Committee (Nagoya, Japan).

Neurological and behavioural testing

The control ($n = 21$) and TDP CKO ($n = 20$) mice were subjected to the Rotarod task (Economex Rotarod; Columbus Instruments) weekly as described previously (Katsuno *et al.*, 2002). Grip strength was measured weekly by a grip strength meter (MK-380M, Muromachi kikai Co. LTD). During this test, the mice griped the mesh with four limbs and their tail was pulled backwards. Gait stride was measured from 50 cm of footsteps, and the average value was recorded for each mouse.

Immunofluorescent analysis and immunohistochemistry

For immunofluorescent analysis, we perfused 20 ml of a 4% paraformaldehyde fixative in phosphate buffer (WAKO Corp.) through the left cardiac ventricle of mice deeply anaesthetized with medetomidine (0.3 mg/kg), midazolam (4 mg/kg) and butorphanol (5 mg/kg), interperitoneally. Tissues postfixed overnight in 10% phosphate-buffered formalin were then processed for paraffin embedding. We then deparaffinized 3 -μm thick tissue sections and dehydrated them with alcohol. Sections were first microwaved for 20 min in 50 mM citrate buffer (pH 6.0), treated with TNB blocking buffer (PerkinElmer) and incubated overnight with anti-TDP-43 rabbit polyclonal antibody (1:1000, ProteinTech), anti-choline-acetyltransferase (ChAT) goat polyclonal antibody (1:100, Milipore), anti-microtubule-associated protein 1 light chain 3 (LC3) mouse monoclonal antibody (1:1000, MBL), phosphorylated neurofilament-H (pNF-H) mouse monoclonal antibody (SMI31) (1:1000, Covance), or anti-neuronal nuclei (NeuN) mouse monoclonal antibody (1:100, Millipore). After washing, for the ChAT staining, sections were incubated with biotinylated donkey anti-goat IgG (1:300, Vector Lab.) for 30 min, washed and incubated with streptavidin conjugated with Alexa Fluor® 546 (1:1000, Invitrogen) for 30 min. For the other antigens, sections were incubated with the indicated secondary antibody and TO-PRO®3 (Invitrogen), a nuclear marker, for 30 min, mounted with ProLong® Gold Antifade reagent (Invitrogen), and then imaged with a laser confocal microscope (LSM710, Carl Zeiss). For immunohistochemistry, sections were incubated overnight with anti-glial fibrillary acidic protein (GFAP) mouse

monoclonal antibody (1:1000, Sigma-Aldrich), stained using the DAKO EnVision™+ HRP system (Dako Corp.) and photographed with an optical microscope (Axio Imager M1). The immunoreactive area in the ventral horn of TDP CKO mice and control littermates at the indicated ages ($n = 3$ for each age) was analysed with WinROOF (Mitani). The binary treatment included application of a staining intensity threshold and size exclusion criteria to distinguish the significant structures from the background signals. All sections analysed were treated with the same threshold and exclusion criteria.

Retrograde FluoroGold neurotracer labelling

Retrograde labelling of motor neurons was performed as described previously (Katsuno *et al.*, 2006). Briefly, a total volume of 4.5 µl of 2.5% FluoroGold solution (Biotium) was injected into the gastrocnemius muscle of anaesthetized mice. Lumbar spinal cords were removed 46 h after FluoroGold administration. The frozen optimal cutting temperature (OCT) compound-embedded samples were sectioned longitudinally on a cryostat at 10 µm and mounted on silane-coated slides. After the FluoroGold labelled motor neurons in the L5 segment was photographed with Zeiss Axio Imager M1 (Carl Zeiss), the sections were fixed with 4% paraformaldehyde, stained with anti-TDP-43 and anti-ChAT antibody, and photographed with LSM710. For the quantification of retrograde labelling, we measured every third section (a total of five sections in L5 ventral horn), and counted the degree of FluoroGold labelling in motor neurons of two control mice, and TDP-43-positive or -negative motor neurons of two TDP CKO mice.

Electron microscopy

Under the deep anaesthesia, 2-year-old TDP CKO mice and control littermates were transcardially perfused with 3% paraformaldehyde and 1% glutaraldehyde in PBS. The spinal cords and sciatic nerves were removed, and postfixed overnight in the perfusing solution. After fixation, the spinal cords were immersed in the solution (0.1 M cacodylic acid, 2% paraformaldehyde, 2.5% glutaraldehyde) for 12 h. The anterior half of lumbar spinal cord was sectioned transversely, postfixed in 1% osmium tetroxide for several hours, dehydrated and embedded in epoxy resin. Each block was cut into serial semithin sections (~1-µm thick). These sections were stained with toluidine blue. Appropriate portions of the sections were cut into ultrathin sections, which were then stained with uranyl acetate and lead citrate. Two-year-old TDP CKO mice and control littermates were analysed. Electron microscopic photographs were obtained under an original magnification of ×5000 and printed at a final magnification of ×9500.

Analysis of muscle, neuromuscular junction and motor axon

To investigate the presence of muscle atrophy, gastrocnemius muscles were dissected free, quickly frozen by immersion in cooled acetone and powdered CO_2. Ten-micrometre thick transverse frozen sections were stained with haematoxylin and eosin. For analysis of neuromuscular junctions, 30-µm thick frozen longitudinal sections of the tibialis anterior muscle were incubated overnight with alpha bungarotoxin conjugated with biotin-XX (1:80, Invitrogen), anti-pNF-H mouse monoclonal antibody (SMI31, 1:100) and anti-synaptophysin rabbit polyclonal antibody (1:100, Cell Signaling Technologies). After washing, sections were incubated with goat anti-rabbit and anti-mouse IgG conjugated with Alexa Fluor® 488 (1:1000 for each, Invitrogen) and streptavidin conjugated with Alexa Fluor® 564 (1:1000, Invitrogen) and mounted with ProLong® gold (Invitrogen). The stained sections were imaged with a laser scanning confocal microscope (LSM710, Carl Zeiss). More than 100 neuromuscular junctions from TDP CKO mice aged 20, 50, 80 and 100 weeks were analysed ($n = 3$ mice for each group). For morphological analyses, epoxy resin embedded transverse sections of L5 ventral roots were stained with toluidine blue. L5 ventral roots of 20, 50 and 100 week-old mice ($n = 6$ axons for each group) were assessed. The diameter of myelinated fibres was automatically measured using a computer-assisted image analyser (Luzex FS), as described previously (Katsuno *et al.*, 2002). Paraffin embedded transverse sections of L4 ventral roots of 100-week-old mice were stained with an antibody against ChAT and photographed by Zeiss Axio Imager M1.

Quantification and morphological analysis of motor neurons

For the quantifications and morphological analyses of motor neurons, we performed the immunofluorescent analyses of the paraffin-embedded sections stained with anti-TDP-43 and anti-ChAT antibodies of L5 spinal cord ($n = 5$ for each) and brain stem ($n = 3$ for each) of control and TDP CKO mice. All the neurons within the every fifth sections from the 50 consecutive sections of lumbar spinal cord, or every third sections from all consecutive sections of brain stem including the each cranial motor nucleus were assessed using AxioVision softwear (Carl Zeiss), after samples were photographed by Zeiss Axio Imager M1 (Carl Zeiss). The ChAT-positive neurons in the ventral horns or cranial nuclei were regarded as motor neurons. We examined the presence of nuclear immunoreactivity for TDP-43 in ventral horns and brainstems, and calculated the TDP-43-knockout efficiencies, the number of remaining motor neurons, and the size of motor neurons in each group. To evaluate the involvement of gamma-motor neuron, we measured the number of large ($>250\,\mu m^2$) or small ($<250\,\mu m^2$) lumbar motor neurons.

Statistical analyses

Statistical differences were analysed by Kaplan–Meier and logrank test for survival rate, ANOVA and Bonferroni *post hoc* analyses for multiple group comparisons and the unpaired Student's *t*-test for two group comparisons (SPSS version 15.0, SPSS Inc.).

Results

Generation of TDP CKO mice

We constructed a TDP-43flox allele by flanking the second exon of the mouse TDP-43 gene (*Tardbp*) with loxP sites (Supplementary Fig. 1A and B). Because the second exon contains the *Tardbp* start codon, Cre-mediated deletion of this exon inhibits mouse TDP-43 translation. To delete TDP-43 expression specifically in motor neurons, TDP-$43^{flox/flox}$ mice were crossed with VAChT-Cre.Fast mice, in which Cre expression is mostly restricted in the postnatal somatomotor neurons (Misawa *et al.*, 2003). The immunofluorescent analysis of the ventral horn from TDP CKO mice at post-natal Day 2 showed that all the assessed motor neurons were positive for TDP-43 (Supplementary Fig. 1C). On

the other hand, the quantitative analysis of the lumbar ventral horn and hypoglossal nucleus from 10-week-old TDP CKO mice showed that TDP-43 was knocked-out in 48% of motor neurons in the lumbar ventral horn and 45% in the hypoglossal nucleus (Fig. 1A and B). In addition, reverse transcriptase PCR analysis of total RNA from motor neurons isolated by laser microdissection, revealed that exon 2 of *Tarbdp* was partially skipped under the Cre expression (Supplementary Fig. 1D and E). Immunoblot analysis showed that the TDP-43 protein expressions in liver, kidney, heart, skeletal muscle and cerebral cortex of TDP CKO mice were not altered compared with their control littermates (Supplementary Fig. 1F). Immunofluorescent analysis of the

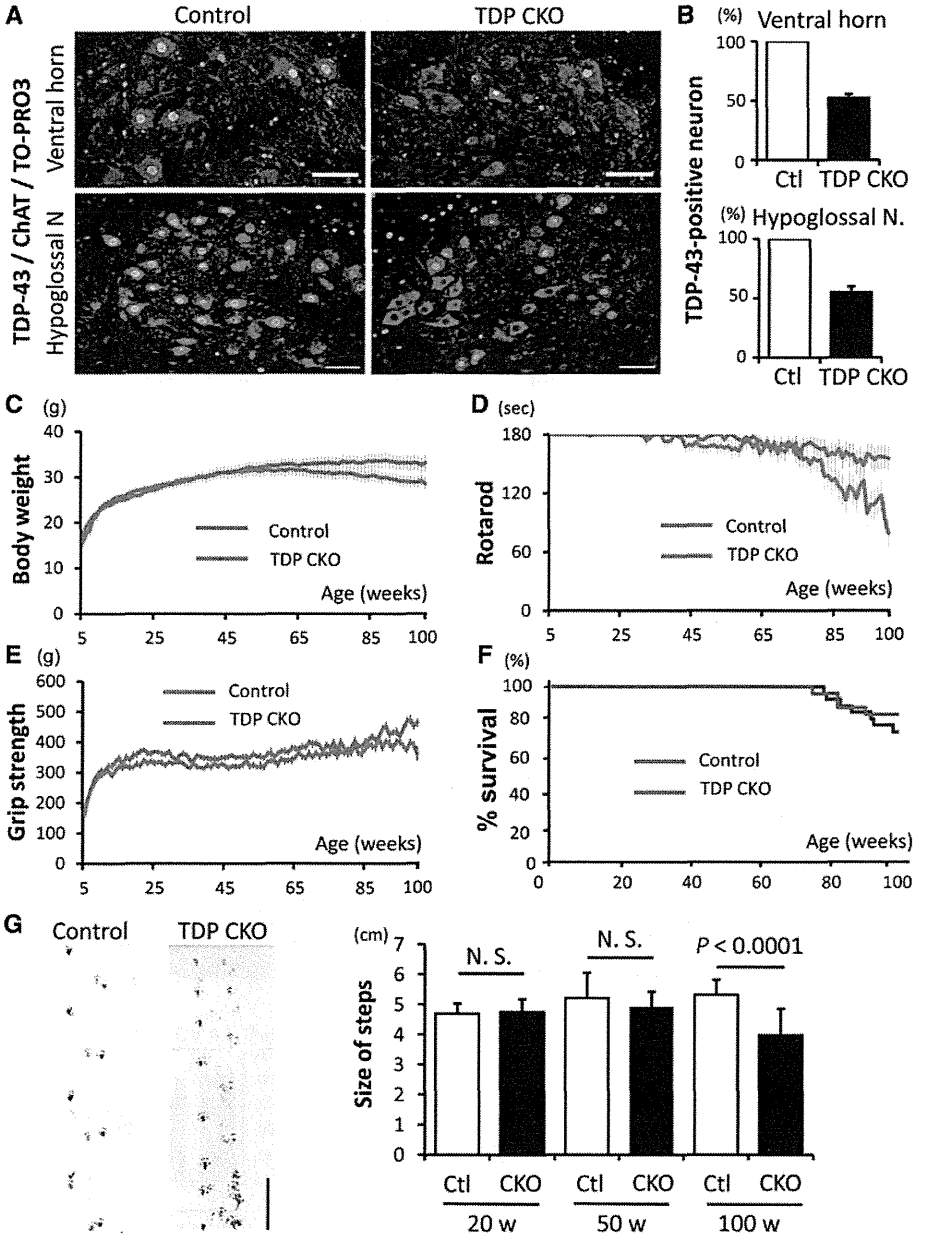

Figure 1 Progressive motor dysfunction in TDP CKO mice. (**A**) Immunofluorescent stainings (TDP-43; green, ChAT; red, TO-PRO3; blue) of lumbar ventral horn and hypoglossal nucleus of 10-week-old control and TDP CKO mice. (**B**) Percentage of TDP-43-positive motor neurons in the lumbar ventral horn and hypoglossal nucleus (N.) of 10-week-old control (Ctl) and TDP CKO mice ($n = 3$ for each group). (**C–E**) Body weight (**C**), Rotarod task (**D**), and grip strength (**E**) phenotypes of control (red line, $n = 21$) and TDP CKO mice (blue line, $n = 20$). Error bars indicate SEM. (**F**) Survival rates of control ($n = 27$) and TDP CKO mice ($n = 26$). (**G**) The average length of hindpaw steps in 20-week-old ($n = 6$ for each), 50-week-old ($n = 6$ for each), and 100-week-old ($n = 15$ for each) control and TDP CKO mice. Error bars indicate SD. Scale bars: **A** = 50 μm; **G** = 5 cm. N.S. = not significant.

lumbar dorsal horn of 10-week-old control, TDP CKO and TDP hCKO mouse showed that all the assessed neurons were positive for TDP-43 (Supplementary Fig. 2). In addition, the analyses of 100-week-old control, TDP CKO and TDP hCKO mice demonstrated that TDP-43 was not excised in the neurons of the primary motor cortex, putamen, deep cerebellar nucleus and cerebellar cortex of TDP CKO or TDP hCKO mouse (Supplementary Figs 3 and 4).

TDP-43 CKO mice develop progressive motor dysfunction

The earliest symptom of motor deficit in TDP CKO mice was tremor, which appeared as early as 50 weeks. TDP CKO mice exhibited progressive weight loss beginning ~60 weeks (Fig. 1C), when muscle atrophy of the trunk and hind limb was detectable. The grip strength and motor performances in the Rotarod task of TDP CKO mice were lower than their control littermates (Fig. 1D and E) beginning at 85 and 75 weeks, respectively. At 100 weeks, TDP CKO mice were significantly different from the control littermates in body weight ($P = 0.04$), rotarod ($P = 0.001$) and grip strength ($P = 0.002$). The average length of hindpaw steps of TDP CKO mice was significantly shorter than that of control littermates in 100 weeks of age ($P = 0.000001$; Fig. 1G). The survival rate of TDP CKO mice, however, was not altered compared with that of control littermates (Fig. 1F). Analyses of TDP-43$^{flox/+}$ and TDP-43$^{flox/+}$/VAChT-Cre (TDP hCKO) mice, which resulted in heterozygous loss of TDP-43 in motor neurons, showed that body weight, Rotarod task, grip strength and length of hindpaw steps were not significantly different between the two transgenic groups (Supplementary Fig. 5A–D).

TDP-43 depletion leads to atrophy of spinal motor neurons

Because TDP CKO mice exhibited progressive motor impairment, we focused on the morphology of spinal motor neurons. The immunofluorescent analysis of the lumbar ventral horn in 100-week-old TDP CKO mice revealed that motor neurons without TDP-43 were significantly smaller than those with TDP-43 and those in control littermates (Fig. 2A–C). Although TDP-43 was knocked-out in 49% of motor neurons in TDP CKO mice, the number of motor neurons in TDP CKO mice did not differ from that in control littermates (Fig. 2D and E). A time course analysis of TDP-43-lacking motor neurons in TDP CKO mice showed that neuronal atrophy was evident at 100 weeks (Fig. 2F). In addition, we measured TDP-43 knockout efficiency in the small ($>250\,\mu m^2$) and large ($<250\,\mu m^2$) lumbar motor neurons. The results showed that there was no difference in the knockout efficiency between the small and large motor neurons (Supplementary Fig. 6A), suggesting that the TDP-43-knockout efficiency in the gamma-motor neurons of TDP CKO mice is similar to that of alpha-motor neurons. The measurement of the average motor neuron number showed that the number of TDP-43-lacking large motor neurons decreased at 100 weeks of age compared with TDP-43-positive motor neurons, whereas the number of TDP-lacking small motor neurons increased, indicating that postnatal deletion of TDP-43 leads to atrophy of the alpha-motor neurons in the aged TDP CKO mice (Supplementary Fig. 6B). This view is supported

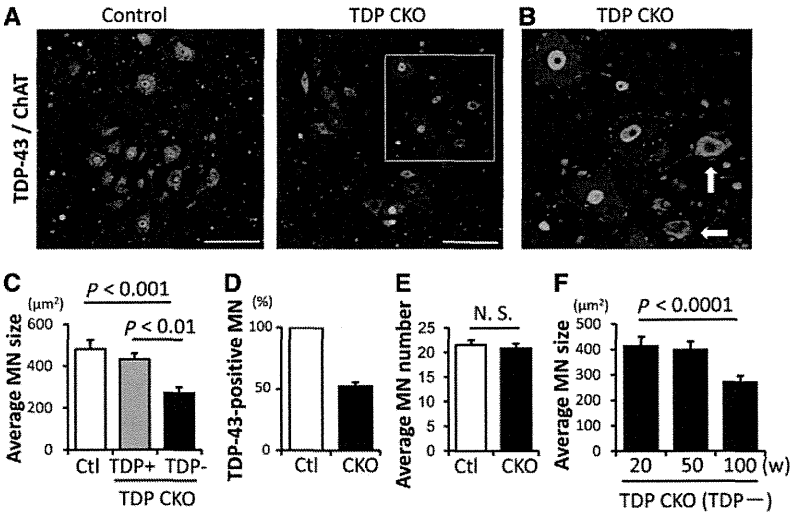

Figure 2 Morphological analysis of spinal motor neurons. (**A** and **B**) Immunofluorescencent stainings (TDP-43, green; ChAT, red) of lumbar ventral horn from 100-week-old control (Ctl) and TDP CKO mice. (**B**) Enlarged image of the area marked in **A** (*left*). TDP-43-lacking motor neurons (arrows) were significantly smaller than TDP-43-positive motor neurons. (**C**) Percentage of TDP-43-positive motor neurons in the lumbar ventral horn of 100-week-old mice ($n = 5$ for each group). (**D**) Average size of spinal motor neurons (MN) in 100-week-old mice ($n = 5$ for each group). Error bars indicate SD. (**E**) Average number of spinal motor neurons in 100-week-old mice ($n = 5$ for each group). Error bars indicate SD. (**F**) Time course of atrophy of TDP-43-lacking motor neurons ($n = 5$ for each age). TDP+ = TDP-43-positive neurons; TDP− = TDP-43-negative neurons. Scale bars = 100 μm.

by the immunofluorescent analysis of the lumbar ventral horn from 100-week-old TDP CKO mice showing that the TDP-43-lacking alpha-motor neuron, which was positive for NeuN and ChAT, was smaller than the TDP-43-positive alpha-motor neuron (Supplementary Fig. 6C). On the other hand, there was no morphological difference in the motor neurons between TDP hCKO and TDP-43$^{flox/+}$ mice (Supplementary Fig. 5E).

TDP-43 depletion affects motor axon, neuromuscular junction and skeletal muscle

The toluidine blue staining of transverse sections of L5 ventral root exhibited axonal degeneration in a subset of large myelinated fibres of TDP CKO mice from 50 weeks (Fig. 3A). Quantitative analyses of the ventral roots demonstrated the decrease of large myelinated fibres and increase of small myelinated fibres in 100 week-old TDP CKO mice (Fig. 3A). The immunofluorescent analysis using anti-ChAT antibody also exhibited the loss of large motor axons in the ventral root of TDP CKO mice (Fig. 3B). Axial sections of the gastrocnemius muscle in 100-week-old TDP CKO mice exhibited grouped atrophy, a neurogenic muscular change (Fig. 3C). Whereas all assessed neuromuscular junctions in the control littermates were innervated, in the TDP CKO mice, the percentage of denervated neuromuscular junctions increased progressively after the age of 50 weeks, concomitant with motor impairment and motor neuron atrophy (Fig. 3D). In analyses of retrograde FluoroGold labelling of the motor neurons in TDP CKO mice, the degree of labelling was significantly less in the TDP-43-lacking motor neurons than in the TDP-43-positive motor neurons (Fig. 3E).

Assessment in motor nuclei of cranial nerves

The histopathology of patients with ALS is characterized by the selective loss of motor neurons with scarcely detectable damage in the extraocular motor nuclei. To examine the region-specific neuropathology in TDP CKO mice, we quantitatively analysed the motor nuclei of cranial nerves. In the trigeminal motor, facial, hypoglossal and abductor nuclei of 100-week-old TDP CKO mice, ~50% of motor neurons were negative for TDP-43, but in the oculomotor nucleus, the efficiency of TDP-43 depletion was only ~25% (Supplementary Fig. 7). Morphological analysis of the trigeminal motor, facial and hypoglossal nuclei in 100-week-old TDP CKO mice revealed that TDP-43-lacking motor neurons were significantly smaller than those with TDP-43 or those of the control littermates (Fig. 4A–C), whereas those in the oculomotor and the abductor nuclei were preserved (Fig. 4D and E), suggesting that this mouse model recapitulates the selective vulnerability of motor neuron in ALS. The time course analysis of the hypoglossal motor nucleus showed that the atrophy of the motor neuron was evident from 50 weeks. The number of motor neurons in these nuclei of TDP CKO mice was not altered compared with the control littermates, as was shown in the spinal cord (Fig. 4A–E).

Astrogliosis in ventral horn and accumulation of phosphorylated neurofilament in motor neurons of TDP CKO mice

Immunohistochemistry of the ventral horn showed that the number of astrocytes progressively increased in TDP CKO mice (Fig. 5A). Phosphorylated neurofilament accumulated in the cytoplasm of TDP-43-lacking motor neurons of TDP CKO mice, but not in motor neurons with TDP-43 in TDP CKO mice or those of control littermates (Fig. 5B).

Formation of autophagosomes in motor neurons of TDP CKO mice

Recent studies indicate that autophagosomes accumulate in motor neurons of patients with sporadic ALS and animal models of motor neuron diseases (Li *et al.*, 2008; Sasaki, 2011; Tian *et al.*, 2011). Therefore, we investigated autophagy-related pathology in 100-week-old control and TDP CKO mice. The immunofluorescent analysis showed LC3-positive puncta in 37% of TDP-43-lacking motor neurons, but not in TDP-43-positive motor neurons in TDP CKO mice or those of the control littermates (Fig. 6A). TDP-43-lacking motor neurons with the puncta were significantly smaller than those without the puncta (Fig. 6B). The ultrastructure of motor neurons from 100-week-old TDP CKO mice demonstrated that autophagy-related structures such as autolysosomes and autophagosomes were accumulated in the cell bodies of motor neurons (Fig. 6C–E), proximal motor axon (Fig. 6F), and sciatic nerve of TDP CKO mice (Fig. 6G–H). These structures were not seen in the control mice as far as we observed.

Discussion

Although TDP-43 is an established pathological hallmark of ALS, it remains unclear how TDP-43 contributes to the pathogenesis. In the present study, we showed that TDP CKO mice, in which TDP-43 was knocked-out specifically in postnatal motor neurons, developed an age-dependent progressive motor impairment such as gait disturbance and muscle atrophy, suggesting that the loss-of-function of TDP-43 in postnatal motor neurons plays a causative role in the neurodegenerative process of ALS. There has been a great deal of debate about whether loss or gain of TDP-43 function causes the neurodegeneration (Lee *et al.*, 2011). Several mouse, rat and primate models overexpressing wild-type or disease mutant TDP-43 recapitulate the phenotype of ALS or FTLD (Wegorzewska *et al.*, 2009; Shan *et al.*, 2010; Stallings *et al.*, 2010; Tsai *et al.*, 2010; Wils *et al.*, 2010; Xu *et al.*, 2010; Zhou *et al.*, 2010; Igaz *et al.*, 2011; Swarup *et al.*, 2011; Uchida *et al.*, 2012); however, redistributions and cytoplasmic inclusions of TDP-43 are generally rare and several models exhibit cytoplasmic mitochondrial aggregation, which is not common in ALS. The expression of endogenous TDP-43 is suppressed in neurons expressing human TDP-43-delta nuclear localization signal as well as those expressing human wild-type TDP-43, suggesting that

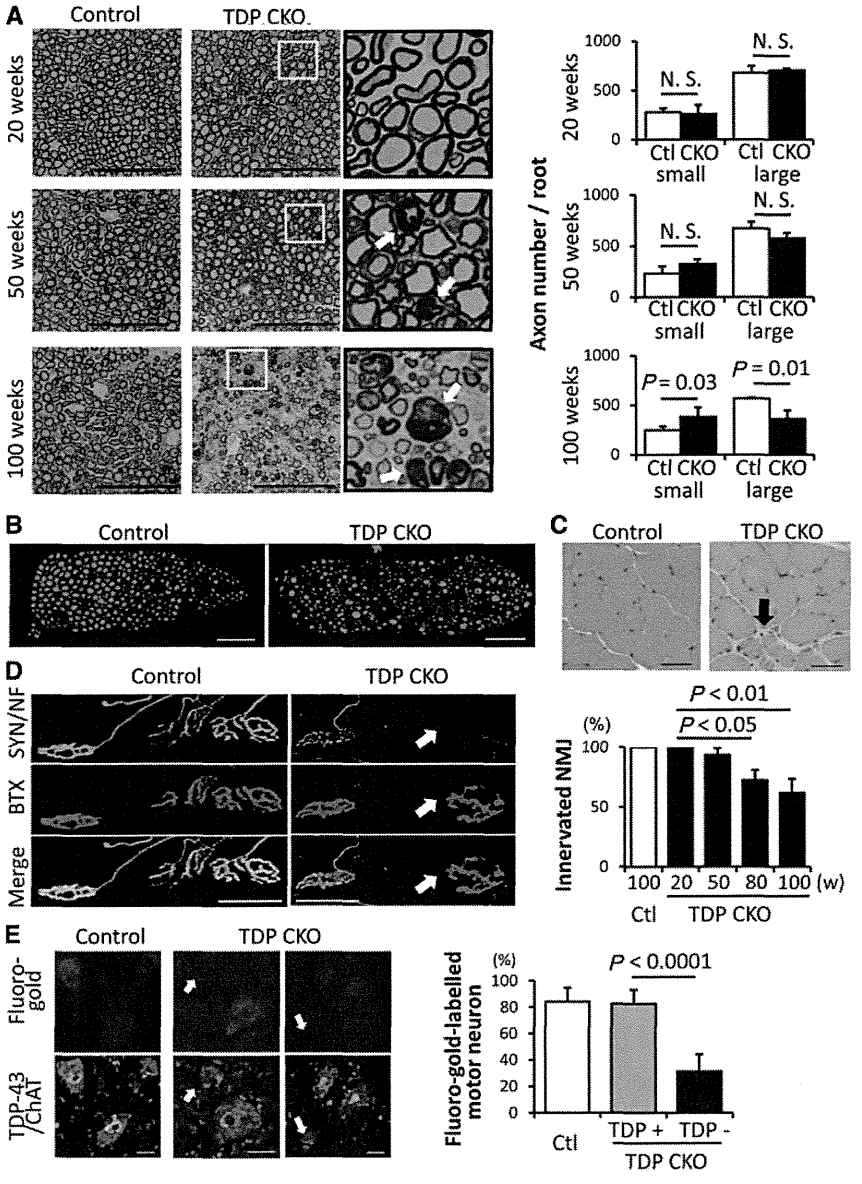

Figure 3 Analysis of motor axons, neuromuscular junctions, and skeletal muscles. (**A**) Toluidine blue staining images and the number of small myelinated fibres (<5 μm) and large myelinated fibres (>5 μm) in the L5 ventral root from 20, 50 and 100-week-old control and TDP CKO mice (n = 6 axons of each). The enlarged image of the yellow-framed area is also shown. Arrows indicate axonal degenerations. Scale bars = 100 μm. Error bars indicate SD. (**B**) Immunofluorescent staining of the L4 ventral root in 100-week-old mice with an anti-ChAT antibody. (**C**) Haematoxylin and eosin staining of gastrocnemius muscles of 100-week-old mice. Axial sections from TDP CKO mice exhibited grouped atrophy (arrow), whereas the control littermates showed no such phenomenon. (**D**) Immunofluorescent staining [synaptophysin (SYN) and phospho-neurofilament (NF), green; bungarotoxin (BTX), red] of neuromuscular junctions (NMJ) in 100-week-old mice and a time course analysis of neuromuscular junctions in TDP CKO mice. Denervated neuromuscular junctions (arrow) are indicated by the lack of synaptophysin and phospho-neurofilament staining. Scale bars = 50 μm. Error bars indicate SD (n = 3). (**E**) FluoroGold labelling (blue) and immunofluorescence staining (TDP-43, green; ChAT, red) of lumbar motor neurons. Retrograde FluoroGold labelling was significantly attenuated in TDP-43-lacking motor neurons but not in TDP-43-positive neurons in 100-week-old TDP CKO mice (arrows). Scale bars = 20 μm. Error bars indicate SD (n = 10).

mutant TDP-43 may cause neurodegeneration through inhibition of normal TDP-43 function (Igaz *et al.*, 2011). On the other hand, TDP-43 knockout mice result in embryonic lethal phenotypes (Kraemer *et al.*, 2010; Sephton *et al.*, 2010; Wu *et al.*, 2010), and systemic postnatal deletion of this molecule led to rapid death (Chiang *et al.*, 2010). Although TDP-43-depleted models of *Drosophila* and zebrafish exhibit neurodevelopmental deficits in motor axons (Feiguin *et al.*, 2009; Kabashi *et al.*, 2011), the

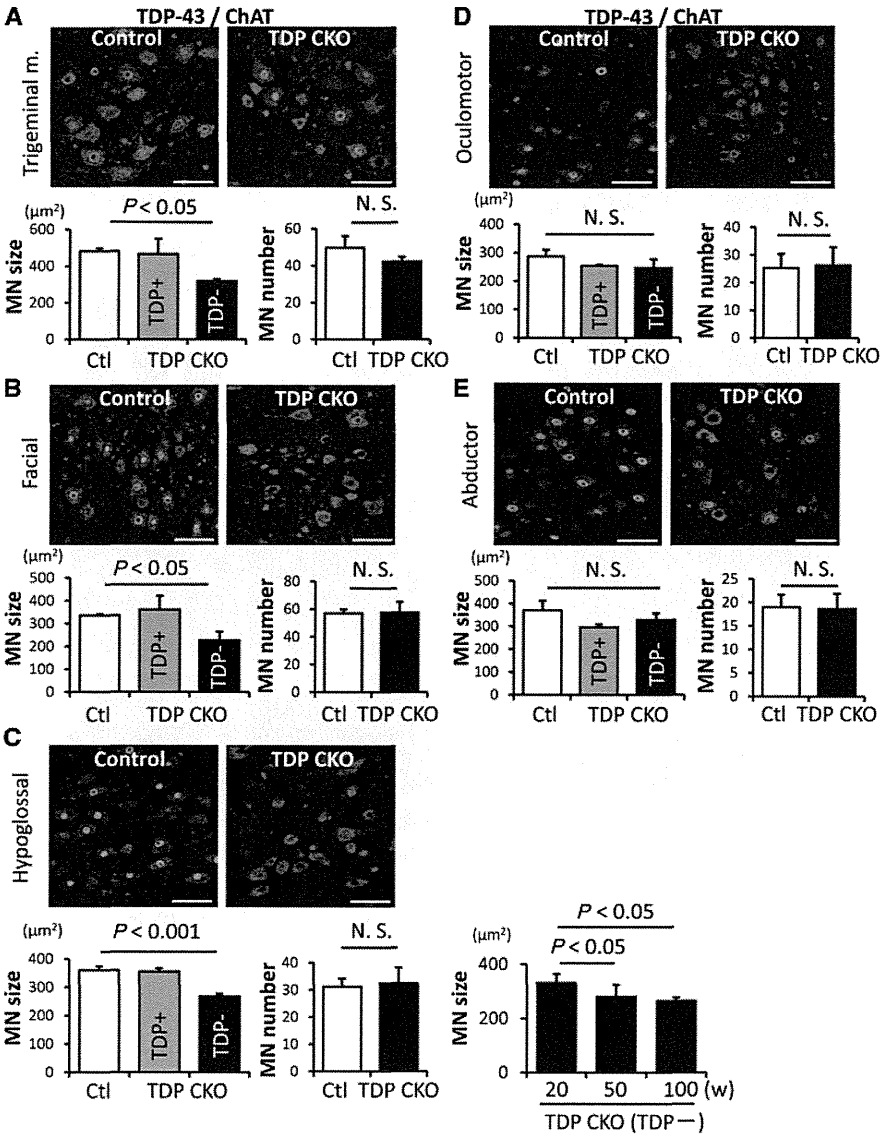

Figure 4 Morphological analysis of cranial motor nuclei. (**A–E**) Immunofluorescent analysis (TDP-43, green; ChAT, red) of motor neurons in the trigeminal motor (m.) (**A**), facial (**B**), hypoglossal (**C**), oculomotor (**D**), and abductor (**E**) nuclei from 100-week-old control ($n = 3$) and TDP CKO mice ($n = 3$). Graphs show the average size and number of motor neurons in each area. TDP+ = TDP-43-positive neuron; TDP− = TDP-43-negative neuron. Error bars indicate SD. Scale bars = 50 μm. MN = motor neuron; N.S. = not significant.

role of TDP-43 in postnatal mammalian neurons has not been fully elucidated. In the present study, we clarified that TDP CKO mice, in which TDP-43 was specifically knocked-out by Cre recombinase in postnatal motor neurons, develops a progressive motor neuronal degeneration as seen in ALS, suggesting that TDP-43 is essential for the long term maintenance of postnatal motor neurons in mice. Although TDP CKO mice developed ALS-like motor impairment, the mortality of the mice was not different from that of control littermates. This might be due to the knockout efficiency of TDP-43, which occurred in ~50% of motor neurons, or due to the life span of mice, which is considerably shorter than the disease duration of patients with ALS. Moreover, there were no significant alterations in body weight, motor function or morphology of motor neurons in our TDP heterozygous CKO (TDP hCKO) mice. Because previous studies demonstrated that the protein expression of TDP-43 was not reduced in various tissues of heterozygous TDP-43 knockout mice (Kraemer *et al.*, 2010; Sephton *et al.*, 2010; Wu *et al.*, 2010), TDP-43 depletion is likely insufficient to affect the motor neurons in our TDP hCKO mice. At the same time, these data suggest that expression of Cre itself did not affect the vulnerability of the mouse motor neurons over 2 years.

An earlier study demonstrates that the motor neuron-specific TDP-43 knockout mouse carrying HB9-Cre exhibits early-onset